5-2010

Implications of Climate-Driven Variability and Trends for the Hydrologic Assessment of the Reynolds Creek Experimental Watershed, Idaho

V. Sridhar
Boise State University

Anurag Nayak
Sutron Corporation

Implications of Climate-Driven Variability and Trends for the Hydrologic Assessment of the Reynolds Creek Experimental Watershed, Idaho

Venkataramana Sridhar
Boise State University

Anurag Nayak
Sutron Corporation

Abstract

The Soil and Water Assessment Tool (SWAT) model was used to assess the implications of long-term climate trends for the hydroclimatology of the Reynolds Creek Experimental Watershed (RCEW) in the Owyhee Mountains, Idaho of the Intermountain West over a 40-year period (1967-2006). Calibration and validation of the macroscale hydrology model in this highly monitored watershed is key to address the watershed processes that are vulnerable to both natural climate variability and climate change and . The model was calibrated using the streamflow data collected between 1997 and 2006 from the three nested weirs, the Reynolds Mountain East (RME) , Tollgate and Outlet. For assessing the performance of the calibrated model, this study used 30 years of streamflow data for the period between 1966 and 1996. This investigation suggested that the model predicted streamflow was best at RME, and inadequate at Outlet. Simulated soil moisture was also verified using the data available from five soil moisture measurement sites. The model was able to capture the seasonal patterns of changes in soil water storage considering the differences in the spatial extent of the observed and predicted soil water storage (point measurements against the spatially averaged values for the HRU) and uncertainty associated with the soil moisture measurements due to instrument effects. Water budget partitioning during a wet (1984) water year and a dry (1987) water year were also analyzed to characterize the differences in hydrologic cycles during the extreme hydrologic conditions. Our analysis showed that in the dry water year , vegetation at the higher elevation were under water stress by the end of the water year. Contrastingly, in the wet water year only the vegetation at low and mid elevations were under water stress whereas vegetation at the at the higher elevations derived substantial soil moisture for ET processes even towards the end of the growing season. To understand the effect of climate change on the hydrologic cycle, the observed and simulated streamflow were analyzed for trends in Center of Timing (CT). Earlier CT timings for the simulated and observed streamflow at RME weir was obvious thus manifesting global warming signals at the watershed scale level in the Intermountain west region. Observed streamflow at the Tollgate and Outlet weirs, where streamflow is partially affected by the agricultural diversions, showed later CT timings and these results appeared to suggest that climate impact assessment studies need to carefully distinguish the system behavior that is altered by both natural and human-induced changes.

Keywords: Hydrologic cycle, climate variability, snow melt, modeling, Reynolds Creek, Idaho

1. Introduction

Precipitation over the intermountain west exhibit a strong seasonal pattern and majority of it falls during the cold winter season as snow with the region normally experiencing hot and dry summer. The Intermountain west in the U.S is bounded by the Rocky Mountains to the east and the Cascades and Sierra Nevada to the west that is punctuated by low and mid-elevation mountain ranges. Generally, regional water management strategies in the U.S. west are based on the amount of snow received in the winter and the timing of snowmelt in the spring to meet the demand for domestic, agricultural, environmental and industrial purposes. By some estimates as much as 50-80% of

the total streamflow in the intermountain west originates from the melting mountain snowpack (Marks et al. 2001; Stewart et al. 2004, 2005). Therefore, accurate understanding of hydrologic processes occurring in the mountain basins is important to formulate sound water resources policies, planning and management decisions in the region. Recent trends inform us warming climate conditions and changes in both observed and predicted hydrologic cycle of the snowmelt dominated regions further amplified the importance of understanding hydrologic processes in mountain basins. Many studies have indicated that low- and mid-elevation mountainous regions including the intermountain west are more sensitive to climate warming than the higher elevations (Mote 2003, 2006; Hamlet et al. 2005; Mote et al. 2005; Regonda et al. 2005).

Mountain basins exhibit a high degree of spatial variability with respect to climate, soils, vegetation and topography. Understanding the hydrologic processes in these mountain environments requires extensive climate data (such as temperature, precipitation, wind speed, solar radiation, humidity), streamflow, soil moisture and surface flux measurements at a high spatiotemporal resolution. Unfortunately field observations in these complex terrains are rarely available and if available they are still of poor quality, and of spatiotemporally low in resolution due to severe weather conditions and inaccessibility. Measurements are especially rare at remote mountain basins (Hamlet et al. 2005) which however, receive significantly more precipitation due to orographic enhancement (Hanson 1982; Cooley et al. 1988).

Since the availability of continuous observational data at high spatiotemporal resolution is limited, studies often rely on hydrologic models to understand and predict the hydrologic behavior of the mountain basins which is yet again challenging for the same reasons. Two of the dominant hydrologic processes, snow cover development and snowmelt, further introduce complexities in the hydrologic modeling of the mountain basins (Luce et al. 1998).

While the interplay between regional hydrology and mountainous climate is recognized, there has been only limited attempt to model the hydrologic behavior of these snow dominated semi-arid mountain basins. Given the importance of snow cover development and snowmelt from these mountain basins, many modeling efforts were only focused on simulation of snow processes (e.g. Tarboton and Luce 1996; Luce et al. 1998; Marks et al. 2002; Winstral et al. 2002). Various studies (Flerchinger et al. 1998; Flerchinger and Cooley 2000) used Simultaneous Heat and Water (SHAW) 1-D model to simulate the water budget within the sub-watershed of Reynolds Creek Experimental Watershed (RCEW). The Soil and Water Assessment Tool (SWAT) model has been used to identify the streamflow patterns from the snowmelt-dominated basins (Fontaine et al. 2002; Lemonds and McCray 2007; Van Liew et al. 2007; Stratton et al. 2009), and other case studies around the world (e.g., Gui and Rosbjerg, 2009; Demirel et al. 2009), however, these studies were either performed for a relatively short time calibration period or have used sparse streamflow and soil moisture data for validation.

The study watershed, RCEW, located in southwest Idaho, provides an ideal setting to understand the hydrologic cycle as it encompasses typical mountainous basin characteristics outlined above. The watershed is densely instrumented with sensors recording a suite of hydrologic and climate data (Figure 1). Hydrologic regime and flow changes in the RCEW like most of the intermountain west, are highly non-stationary and experience alternating wet and dry cycles unpredictably (Cayan et al. 1999; Newman et al. 2003; Cook et al. 2004).

Temperature over the intermountain west have increased by 1-2 °C over the last 50 years (Trenberth et al. 2007). Numerous studies have demonstrated that the rise in temperature could cause significant changes in hydrology of the snow dominated regions including rain-on-snow events, declining mountain snowpack and earlier snowmelt timings (Mote 2003, 2006; Stewart et al. 2004, 2005; Mote et al. 2005; Hamlet et al. 2005; Regonda et al. 2005). Nayak et al. (2008a) have reported an increase in temperature of ranging from 0.8-2.5 °C and associated phase changes in precipitation from snow to rain, and shift in the timing of runoff in RCEW based on the analysis of 45 years (1962-2006) of observational hydro-climate data.

Assessment of the hydrologic behavior of RCEW involves both quantification of the water budget as well as characterization of the highly variable water balance components influenced by orographic effects, natural climate variability (wet-dry cycles) and the changes associated with warming climate conditions. The Soil and Water Assessment Tool (SWAT) simulates surface and subsurface hydrological processes effectively combining terrain and climate drivers. This research is focused on quantifying the long-term hydrologic behavior by partitioning the water balance into evapotranspiration, runoff, drainage and soil moisture for the period between 1967 and 2006. The specific objectives addressed in this research are: calibrate the surface water flow and snowmelt processes of the

SWAT model using high-resolution precipitation and temperature data for the three sub-basins sequentially to understand the long-term hydrologic budget in RCEW; investigate the spatial and temporal variability of the water balance components and study the changes with regard to the advancement of spring season snowmelt, due to the warming trends as observed from the historical records.

Description of our investigation is organized into the following six sections (a) calibration of the SWAT model using the streamflow data collected from multiple sites within RCEW for the period between 1997-2006, (b) validation of predicted streamflow for the three gage locations using 30-years of observed streamflow between 1967-1996, (c) model performance verification in predicting soil moisture at five sites, (d) spatial variability in the water balance components as a result of land use and elevation changes, (e) natural variability in streamflow caused by the phase shift in the wet-dry cycles and (f) shifts in the timing of peakflow due to alterations in the snowmelt dynamics over the modeling period.

2. Study area: The Reynolds Creek Experimental Watershed

RCEW, a 239 km^2 watershed, located in the Owyhee Mountains of southwest Idaho, was added to the U.S. Department of Agriculture, Agricultural Research Service watershed program in 1960 and continuous measurements of a suite of hydroclimatic records are available for RCEW since early 1960s (Robins et al. 1965; Seyfried et al. 2001). The topography of RCEW ranges from a flat valley in the north to steep mountain slopes in the south, with a range of elevation from 1099 to 2244 m (Figure 1). Perennial streamflow originates from the higher elevations of the basin where snowmelt is the primary source of water supply (Seyfried et al. 2001). Reynolds creek is a third-order perennial stream that flows from south to north and drains to the Snake River (Slaughter et al. 2001). Soils at RCEW are highly heterogeneous with most of the watershed has steep, rocky, shallow soils, but deep, loamy soils can also be found at few high elevation areas where forest communities dominate the land surface (Slaughter et al. 2001; Seyfried et al. 2001). About 77% of the land within the watershed is publically (federal and state) owned and managed by the Bureau of Land Management (BLM).

RCEW represents typical climatic conditions akin to the vast landscapes of the intermountain west. Orographic effects lead to an increase in precipitation and a decrease in temperature with elevation over RCEW. High elevations of the RCEW receive 4-5 times more precipitation than that of the low elevations (Hanson 1982, 2001; Cooley et al. 1988). Snow is the dominant form of precipitation at higher elevations while rain becomes dominant at lower elevations and valley locations of the watershed (Hanson 2001; Nayak et al. 2008a). Land cover in the watershed consists of rangeland (4.3%), sagebrush (83%), deciduous (5%) and evergreen forest (2%) and irrigated cropland (4.7%). Crops grown in the watershed include hay and alfalfa and hey and they are irrigated, but are flood-irrigated from diversion ditches which extract water from the main stem of Reynolds Creek. Forest communities of mountain sagebrush, aspen and conifers are mostly found at high elevations that receive relatively higher snow accumulation. Rest of the watershed is dominated by sagebrush-grassland plant communities.

3. Hydroclimate data

Currently field monitoring at the RCEW is undertaken with 26 precipitation stations, 32 primary and 5 secondary meteorological measurement stations, 9 weirs and 8 soil moisture and temperature measurement sites (Marks et al. 2006). Detailed description of each of the data types used in this study is presented in the following sections.

a. Precipitation

We used the data collected from 14 precipitation stations in this study (Figure 1). These stations were selected based on the period of record and continuity of precipitation data measurements (Table 1). Systematic and mechanical errors encountered by the precipitation gauges due to extreme climatic conditions and high wind speeds are common in the study area. Therefore, precipitation data was carefully preprocessed for mechanical errors (Nayak et al. 2008b) and then corrected for systematic errors using dual gauge technique (Hamon 1971, 1973; Hanson et al. 2004).

b. Daily Maximum and Minimum Temperatures

Measurement of daily maximum and minimum temperatures (hereafter Tmax and Tmin, respectively) from three climate stations, located at low (site: 076), mid (site: 127) and high (site: 176) elevations of the watershed were used for our purpose. Additional measurements from these stations include solar radiation, relative humidity, wind speed and wind direction. Detailed description of climate database at RCEW can be found elsewhere (Hanson et al. 2001; Flerchinger et al. 2007). However, we have only used Tmax and Tmin data collected from these three sites in order to maintain consistency with the input data used over the entire duration of study.

c. Streamflow

Streamflow data collected from three long-term stream gauges, namely the Reynolds Mountain East (RME), Tollgate and Outlet was used for model calibration and validation (Figure 1 and Table 2). Details on the location, elevation, drainage area and the length of measurement records for these streamflow gauges are shown in Table 2. Observed streamflow manifested strong signatures of spring snowmelt with peak flows occurring in May across the watershed. Streamflow at RME, the headwater catchment, is strongly driven by the spring snowmelt and as much as 80-95% of total annual streamflow occurs due to spring snowmelt between April and June (Figure 2a). Streamflow at the two downstream locations, Tollgate and Outlet showed relatively more uniform flow due to increased contribution of streamflow generated from rain and rain-on-snow events (Figure 2b and 2c).

d. Soil Moisture

Biweekly measurements of soil moisture content at multiple depths recorded using neutron probe access tubes at five sites were available for our study. Site distribution in the watershed include: two low elevation sites (057 and 076); two mid elevation sites (098 and 127); and one high elevation site (176) that represent different climate zones, topography and land cover (Figure 1). Measurements were made at depths of 15 cm and 30.5 cm followed by readings at 30.5 cm intervals to the bottom of the access tube. Maximum depth of the access tubes ranged from 61 cm to 274 cm (Seyfried et al. 2001). Seyfried et al. (2001) demonstrated that despite the replacement of sensors and the bias introduced thereafter, absolute change in soil water storage in the soil column was in good agreement with changes in soil water storage measured at the nearby lysimeter. Therefore, we compared the measured change in soil water storage at five soil moisture measurement sites against the modeled change in soil water storage to evaluate the model performance in predicting other water balance components.

e. Spatial Data

Input spatial layers of elevation and land cover were obtained from the RCEW geographic database at 10x10m spatial resolution. We used the maximum likelihood vegetation map derived by digitizing Landsat thematic mapper image based on field surveys and aerial photographs (Seyfried et al. 2001) as the base land cover map. The land use layer was reclassified to match the land use classes defined in the SWAT database (Figure 3).

The STATSGO soil layer was used to derive the soil layer (Figure 4). The STATSGO soil database is used instead of SSURGO because it can be directly processed by the ArcSWAT interface to generate required soil parameter files. SSURGO provides a higher resolution and more detailed soil database than STATSGO but the higher resolution tends to increase computational requirements of the model. Prior studies comparing SWAT simulation results with SSURGO and STATSGO databases do not show any significant difference in the model predictions (Wang and Melesse 2006; Peschel et al. 2006).

3. Methods

a. Description of SWAT

SWAT is a physically based, continuous, distributed parameter model that operates on a daily time-step (Arnold et al. 1998). SWAT models the entire hydrologic cycle, including surface flow, lateral flow, evapotranspiration, shallow infiltration, deep percolation and ground water flows. Input data for the model include spatially distributed information on basins topography, soil properties and land use/land cover along with the time series of forcing hydroclimate data.

SWAT is a computationally efficient model. It subdivides a watershed into sub-basins connected by a stream network. Each sub-basin is then divided into multiple Hydrologic Response Units (HRUs) consisting of area with similar soils, land use and slope. By aggregating the areas of similar soil, land use and slope into a single HRU, the model reduces computational requirement significantly with minimal effects on the spatial heterogeneity of the watershed processes.

Simulation of the hydrologic cycle in SWAT can be separated into two major phases, land phase and routing phase. Land phase of hydrologic cycle in SWAT is based on the water balance equation (all units in mm):

$$SW_t = SW_0 + \sum_{i=1}^{t}\left(R_{day} - Q_{surf} - E_a - w_{seep} - Q_{gw}\right) \quad \text{----------(1)}$$

Where SW_t is the soil water content after t days, SW_0 is the initial soil water content, R_{day}, Q_{surf}, E_a, w_{seep}, Q_{gw} are precipitation, surface runoff, evapotranspiration, water entering vadose zone, and return flow respectively on day i (Neitsch et al. 2005). Precipitation is the primary input to the hydrologic cycle. SWAT provides a number of unique options for estimating all of the other water balance components. Q_{surf} can be computed either by the Soil Conservation Service Curve Number (SCS-CN; USDA-SCS 1972) technique or by the Green-Ampt Mein-Larson (GAML) infiltration (Green and Ampt 1911; Mein and Larson 1973) method. E_a can be estimated by three methods in SWAT: the Hargreaves (Hargreaves and Samani 1985), the Priestley-Taylor (Priestley and Taylor 1972) and The Penman-Montieth (Penman 1956; Montieth 1965) method. Water entering into the soil can move along several different pathways. The water in the vadose zone can be: removed from the soil by evaporation or plant water uptake, percolate deep to recharge aquifer or move laterally in the profile to contribute to streamflow. SWAT models Q_{gw} in terms of ground water balance. SWAT simulates two aquifers: a shallow aquifer that contributes to streamflow in the main channel or reach and a deep aquifer that contributes to streamflow somewhere outside the basin.

Routing of water though the reaches or main channel in SWAT is defined as open channel flow. SWAT uses Manning's equation to define the rate and velocity of flow. Water is routed through the channel network using the variable storage routing method (Williams, 1969) or the Muskingum River routing method. SWAT uses a temperature index-based approach to define snow processes. Precipitation on a given day is assumed to be snow if daily average temperature is less than the snowfall temperature threshold (SFTMP). Snowpack temperature lag factor (TIMP) defines snowpack temperature based on daily average air temperature and previous day snowpack temperature. Snowmelt in SWAT is calculated as a linear function of the differences between the average of daily Tmax -snowpack temperature and the snowmelt temperature threshold (SMTMP). Melt factor for any given day is calculated based on maximum (SMFMX) and minimum melt rates (SMFMN) occurring on summer and winter solstices, respectively. The areal distribution of snow cover and melt rate was also improved by the introduction of areal snow coverage distribution curve. This curve is defined by the maximum snow cover at 95% snow cover (SNOCOVMX) and at 50% areal snow cover extent (SNO50COV). The shape of the depletion curve defines the total melt water produced based on the total areal snow cover of the basin. This improved snowmelt algorithm has been used successfully for hydrologic predictions in snowmelt dominated basins (Fontaine et al. 2002; Lemonds and McCray 2007; Zhang et al. 2008; Stratton et al. 2009).

b. Model Setup

The most recent version of the SWAT model, SWAT-2005, along with an ArcGIS interface (ArcSWAT; Olivera et al. 2006) was used in this study. The simulation was performed at a daily time step. For monthly and annual water balance analysis, we aggregated the daily simulation results and it is discussed in the results section. ArcSWAT interface extracts hydrologic information from spatial data (delineates sub-basins, streams, reaches and HRUs), assigns parameter values based on soil and vegetation coverage, and uses it for preparing SWAT input files.

Modified SCS-CN technique was used to estimate surface runoff. SWAT also provides the option of using more physically based GAML approach for infiltration computation but it requires hourly precipitation data. SCS-CN technique estimates runoff based on soil properties, soil moisture conditions, land use and management practices. Hargreaves method was used for estimation of evapotranspiration because it only requires daily Tmax and Tmin for calculating ET. However, more physically based Priestley-Taylor or Penman-Montieth methods for ET estimation are available within the model but these methods require additional data of solar radiation, relative humidity and wind speed which were not available for the entire modeling period.

For each sub-basin, a single weather station is enough to represent the basin meteorology and it is based on its proximity to the centroid of the sub-basin to distribute the forcing data. This type of spatial distribution of weather variables to populate the subbasin may not be ideal for the mountainous basins where both precipitation and temperature vary with elevation rapidly,. However, Fontaine et al. (2002) modified SWAT snow routine which allows 10 elevation bands for each sub-basin for better distribution of precipitation and temperature over the mountainous basins.

First step for an accurate distribution of precipitation and temperature data was to identify the lapse rates for precipitation and temperature. At RCEW, average temperatures generally decrease with increase in elevation and the temperature lapse rates are spatially and temporally variable. The difference in temperature between low and high elevation sites vary between 4 °C/km in the winter to 7 °C/km in the summer (Hanson et al. 2000). Hanson et al. (2000) also reported that there is a mean annual temperature gradient of -2.2 °C/km between low and mid elevation stations and a gradient of -7.2 °C/km between mid and high elevation climate station. This difference in temperature gradient is caused by the cold air drainage to the valley region of the watershed which results in colder temperatures, especially Tmin, at the low elevation site.

Current SWAT setup does not provide the option of specifying seasonally variable lapse rates. Although separate lapse rates can be specified for each elevation band for every sub-basin, we decided to use one single lapse rate for the entire RCEW. The use of single lapse rate is justified because inversion normally occurs on clear days and therefore cloudy days (and the days with precipitation) that are hydrologically more important remain unaffected by the inversion. Regression analysis of the mean annual temperature performed over the three climate stations yielded an annual temperature lapse rate of -0.005 °C/m (Figure 5a). Therefore, a temperature lapse rate of -5 °C/km was used to distribute temperature over the watershed. This temperature lapse rate was comparable with the temperature lapse rates used in the previous studies over the mountain catchments (e.g. Fontaine et al. 2002; Lemonds and McCray 2007, Stratton et al. 2009).

Snow cover development and snowmelt play a critical role in the hydrological processes of RCEW. As typical of the mountainous basins, RCEW not only exhibits orographic enhancement in precipitation with elevation but also experiences substantial differences in precipitation between the leeward and windward sides of the watershed. Precipitation events are normally crossing the watershed from west-southwest direction and thus leeward slopes along with the west and southwest sides of the watershed receive more precipitation than the north and east slopes (Hanson, 2001).

The distribution of snow deposition and melt is important in order to accurately represent the hydrologic processes of RCEW (Flerchinger et al. 1998; Marks et al. 2002; Winstral and Marks 2002). Based on our understanding of the distribution of precipitation over the watershed, we used two separate precipitation lapse rates for leeward and windward slopes instead of using a single lapse rate for the entire watershed and to our knowledge this unique approach has been demonstrated for the first time in mountainous settings. Regression analysis resulted in the annual precipitation lapse rates of 0.86 mm/m and 0.78 mm/m, respectively for leeward and windward sides (Figure 5b). However, as precipitation lapse rates are applied over the daily precipitation data, computed annual lapse rates are assumed to be true at the daily time step and hence the daily lapse rates of 0.86 mm/km and 0.78 mm/km were used for leeward and windward sides, respectively.

c. Sensitivity analysis and calibration

SWAT uses physically-based equations to model the entire hydrologic processes of a watershed. These equations are characterized by a multitude of parameters which are nonlinearly related and identifying optimal parameters can be a challenge due to spatial variability, measurement errors, cost constraints etc. Therefore, model calibration is often critical to identify optimum values for the set of parameters and to improve the predictive power of the model.

As multiple parameters are used in SWAT to define the hydrologic characteristics of the watershed, calibration of all of them is not only time consuming but also not practical. Therefore, it is important to identify the most sensitive model parameters for calibration and that can be accomplished by choosing certain hydrological processes that are most relevant to the study area. SWAT interface incorporates the Latin Hypercube One-At-a-Time (LH-OAT) method to assess the relative sensitivity of the model parameters (Van Griensven et al. 2006). The LH-OAT method first divides the parameter space into a number of Latin Hypercube (LH) sampling intervals and then varies each of

the parameters one at a time for each of the LH sampling interval. The LH-OAT method was used to evaluate the relative sensitivity of the 28 flow parameters by varying them over defined ranges.
Since the start of hydrologic measurements in early 1960s, the quality of hydroclimate measurements to quantify the hydrologic responses of the RCEW has improved constantly due to advancements in sensor technology and increased awareness and the need for understanding of hydrology-climatology interactions. Climate at RCEW is highly variable and subject to wet and dry precipitation cycles (Cayan et al. 1999; Cook et al. 2004). Therefore, a ten-year period between 1997 and 2006 was selected for calibration. This period falls in the tail end of the modeling period when the data quality is good and the study area experienced average, wet and dry hydrologic conditions. However, using the split sampling approach, we identified a non-calibration period, i.e. 1967-1996 for validation of the model results.

Streamflow generation patterns in the RCEW changes rapidly between the snowmelt-dominated upper watershed and the rain-dominated lower watershed. Therefore, relative importance of hydrologic processes change from high to low elevations of the RCEW. For our simulation of the hydrologic cycle of the RCEW, the model was calibrated separately at each of the long-term weirs discussed earlier. Calibration was first performed at the uppermost sub-basin using the RME weir and the parameters were fixed. Subsequently, the downstream watershed that drains at the Tollgate weir was calibrated leaving the RME watershed calibration unaltered and finally the entire watershed that drains at the Outlet weir was calibrated without affecting the upper two sub-basins calibration that was completed previously.

Streamflow pattern measured at the RME weir is strongly seasonal and is primarily driven by the spring snowmelt during the months of April to June. For the RME sub-basin, we calibrated the model separately for the snowmelt-dominated high flow periods and low flow periods. Given the physical setting, the amount and pattern of snow distribution and observed hydrology of the RME sub-basin, it is normal to expect the ranking based on the sensitivity of the snowmelt parameters within SWAT should be higher. However, for unknown reasons the parameters pertaining to the snowmelt processes, except TIMP, were not ranked high.

Therefore, values for all snowmelt parameters, except TIMP, were selected based the literature and manual calibration so that the simulation results best match the observed pattern of streamflow at the RME weir. Optimum value for TIMP was selected based on auto-calibration along with other selected sensitive parameters as described below. The selected values of snow parameters are presented in Table 3 and it includes the lower, the upper and optimized values. Because the snowmelt parameters are basin-scale parameters, they were not adjusted in the subsequent model calibrations.

After adjusting the model parameters for the snowmelt periods, six most sensitive parameters (including TIMP) were selected for calibration with the streamflow data from the RME sub-basin. Calibration of these model parameters was done using the shuffled complex evolution (SCE) algorithm (Duan et al. 1992). The SCE method integrated into SWAT provides options for selecting one of the two objective functions: the sum of the squares of the residuals (SSQ) and the sum of the squares of the differences after ranking (SSQR). The SSQ method aims at minimizing the difference between simulated and measured time series while the SSQR method aims at matching the frequency distribution of the observed and simulated series. The approach involving minimization of SSQ was selected as the objective function for calibration in this study because the SSQR method does not account for the time of occurrence of a given variable which is essential for the hydrological variables. The calibrated parameters and their optimized values are presented in Table 4.

For the calibration middle sub-basin with an outlet at Tollgate, the most sensitive parameters were identified initially. Subsequently, the parameters that affect surface flow (CN2, CANMX, and ESCO) were calibrated to approximate high flows while groundwater flow parameters (ALPHA_BF, GWQMN, RCHR_DP, and REVAPMN) were adjusted to approximate low flows. After obtaining the approximate parameter values using manual calibration, automated SCE algorithm was again used to find the best parameter values within the tight parameter space near the manually calibrated parameter values. Table 5 presents the information of the calibration parameters for the Tollgate weir sub-basin. Finally, the model was calibrated using streamflow measurements at the downstream point, namely Outlet, without changing the parameter values for the above two sub-basins. The method was identical to the earlier two sub-basin calibration. The calibrated parameters and their optimized values for the Outlet weir are shown in Table 6.

The following sections describe the predictive performance of the calibrated model. Model simulated streamflow and soil moisture was validated by comparing with the observed streamflow at three all three gauges for the period between 1967 and 1996. This study also used the long-term soil moisture measurements from five sites across the watershed to validate the predicted changes in the soil water storage for the HRUs in which these sites are located.

d. Statistical analysis of model performance

Five statistical indicators were used to evaluate the predictive performance of the model. These statistical indicators are: the Nash-Sutcliffe coefficient of efficiency (NSE; Nash and Sutcliffe 1970), root mean squared errors (RMSE), the percent deviation from observed streamflow (PBIAS), the coefficient of determination (R^2) and the slope of the regression line. Equations for each of the indicators are given below:

$$NSE = 1 - \frac{\sum (O - P)^2}{\sum (O - \bar{O})^2} \qquad \text{----------(2)}$$

$$RMSE = \sqrt{\frac{\sum (O - P)^2}{n}} \qquad \text{----------(3)}$$

$$PBIAS = \frac{\sum (O - P)}{\sum O} \times 100 \qquad \text{----------(4)}$$

$$R^2 = 1 - \frac{\sum (O - P)^2}{\sum (O - \bar{O})^2} \qquad \text{----------(5)}$$

$$Slope = \frac{\sum (O - \bar{O})(P - \bar{P})}{\sum (O - \bar{O})^2} \qquad \text{----------(6)}$$

where O is the observed values, P is the predicted values, $\bar{O}$ is the mean of observed values, P is the mean of predicted values and n is the number of data records. The NSE values range from $-\infty$ to 1. An NSE value of 1 indicates a perfect agreement between the observed and predicted values while a value of 0 indicates that the model is a good predictor of observed values as $\bar{O}$ and negative values indicate that the $\bar{O}$ is a better estimator than the model. One of the problems with NSE is that it overemphasizes large flows relative to other values by squaring the deviations (Criss and Winston 2008). Also NSE values do not indicate whether the model is over predicting or under predicting the observed values. The RMSE value, a measure of total magnitude of error between observed and predicted values. The PBIAS values indicate whether the model is over predicting or under predicting the observed value. Optimal value for PBIAS is 0; with negative values indicate over prediction and positive values indicate under prediction. The R^2 statistics is a statistical measure of how well the simulated values correlate with the observed data points and a value of 1 represents a strong linear relationship between the observed and predicted values while a R^2 value of 0 indicate no linear relationship between observed and predicted values. Slope of the regression line indicates the nature of correlation between observed and predicted values. An optimum value for slope is 1 which represents that the changes in predicted values are proportional to the changes in observed values.

4. Results and Discussion

We evaluated the hydrologic components predicted by SWAT over the 40-year period. This section reports the results of (1) the model calibration and validation using measured streamflow from RME, Tollgate and Outlet streamflow gauges, (2) model validation based on the measured change in soil moisture storage at five soil moisture measurement sites, (3) spatial variability of the water balance components due to gradients in elevation and vegetation, (4) variability in the watershed behavior due to natural climate variability, and (5) long term changes in streamflow patterns as a result of observed warming over the period of simulation.

i). Model calibration and validation

a. Streamflow

Figures 6(a) and 6(b) present the comparison of the simulated and observed monthly streamflow for both calibration (1997-2006) and validation (1967-1996) phases. A summary of the model performance statistics for the simulated streamflow are presented in Table 7. Visual inspection of the observed and predicted streamflow hydrographs as well as the statistical analysis indicated that the model performed very well in all three gauge locations.

The results indicate that the model performance in predicting streamflow was superior at the headwater catchment, RME, where the model performance statistics for the calibration phase (1997-2006) were NSE = 0.90, Pbias = 5.81%, R^2 =0.90 and slope = 0.95 and for the validation phase (1967-1996) were NSE = 0.89, Pbias = 7.88%, R^2=0.90 and slope = 0.91. Based on these statistics, the model performance is very good in predicting streamflow at the RME sub-basin.

Although the model performance is slightly inferior at Tollgate, the ability of the model in capturing the flow was very good for both calibration (NSE = 0.84, Pbias = -9.44%, R^2 = 0.87, and Slope = 1.02) and validation (NSE = 0.82, Pbias = -12.67%, R^2 = 0.85, and Slope = 1.00) phases.

Model performance was the poorest at Outlet where the model overpredicted streamflow. However, the overall model performance in predicting streamflow at the Outlet weir was still considered good and model performance statistics for both calibration (NSE = 0.70, Pbias = -26.67%, R^2 = 0.82 and Slope = 1.08) and validation (NSE = 0.68, Pbias = -10.87%, R^2 = 0.71 and Slope = 0.85) phases were acceptable given the complexities of the hydrological processes at this basin and uncertainty associated with the streamflow measurement at the Outlet weir. During calibration an underestimation by the model with PBIAS of -26.67% , suggests that simulation in dry years for most of the decade resulted in lower streamflows when extraction for irrigation was believed to be at the normal level. This appeared to be causing a higher discrepancy.

The RME is a small experimental watershed (0.39 km^2) and the spatial variability due to changes in elevation, topography and vegetation is comparatively smaller than the large mountainous basins. At RME, approximately 70% of the total precipitation falls as snow (Nayak et al. 2008a) and streamflow is dominated by the spring snowmelt. Therefore by calibrating the model separately for the snowmelt processes, we were able to predict both the timing and volume of snowmelt. At the RCEW, generally streamflow originates from the higher elevations. Streamflow generated from the headwater catchments of the watershed is critical for the sustenance of the regional ecosystem as it provides water during the warm and dry summer.

The middle and lower sub-basins (Tollgate and Outlet) have larger drainage areas (55 km^2 and 238 km^2, respectively) and exhibit greater spatial heterogeneity when compared with the RME sub-basin. Both rain and rain-on-snow events are more frequent at low to mid elevations of the RCEW. During the rain-on-snow events, turbulent transfer of sensible and latent energy can produce substantial snowmelt (Marks et al. 1998, 2001). While the temperature-index method used in SWAT does not capture the physics of turbulent transfer of energy to the snowpack during rain-on-snow events, proper representation of rain-on-snow events including the rainfall intensity, areal extent and duration were not available to drive the model.

The model was substantially overpredicting streamflow at Outlet. Further analysis of the observed and simulated streamflow data showed that the model was significantly underpredicting streamflow during the wet water years: 1972, 1982, 1983 and 1984. These years were very cold and snowy years with greater than average precipitation. As mentioned earlier, precipitation gauge measurements, especially for snow in these environments are affected by the systematic errors due to wind because of which precipitation gauges records less precipitation than actual. A significant undercatch of snow as much as 50-90% of the actual precipitation (Hamon 1973, Hanson et al. 2004) is common in the watershed. Although we used the wind-adjusted precipitation to drive the model, uncertainty in measurement of precipitation may also be responsible for the underestimation during these years. It is also possible that the model may be simulating higher than actual soil moisture storage and ET rates during these years due to greater availability of water. However, model was mostly overpredicting streamflow. The over-prediction was especially significant during the dry water years. This overprediction may partially be due to diversion of water for

agriculture which is unknown and it is reasonable to assume that it was greater during the dry years than the wet years. Overpredictions can also be attributed to few factors including the difficulty in accurately distributing the precipitation as well as the spatial resolution and accuracy of soil and vegetation layers.

About three-forth of the watershed area is under public ownership which is managed naturally. Most of the privately owned areas are located in the valley region and used for agriculture. Streamflow at the RME watershed was completely unaffected by the human activities. Over the Tollgate subbasin only a fraction of streamflow is diverted for agricultural purposes as most of the agricultural lands are located in low elevation regions located downstream of this area. However, streamflow at the Outlet weir might have been significantly affected by the withdrawal of water for irrigation. Overprediction of streamflow at the Outlet weir can also be partially attributed to the diversion of water for agriculture. Since no records were available on diversion and return flows due to abstractions, the measured streamflow used in this study is not natural and it partly explains the discrepancy in the simulated and measured streamflow.

b. Soil Moisture

At RCEW, soil moisture content is measured at five sites using neutron probe access tubes at biweekly interval (Table 1). We extracted the simulated daily soil moisture content from the HRUs within which these five soil moisture measurement sites are located to enable the comparison between the predicted and observed soil moisture content. To compare the spatially-averaged soil moisture content in each HRU with the observed soil moisture content, we calculated the changes in soil water storage from the monitoring sites and for the HRUs in which these sites are located following the procedure described by Seyfried et al. (2001). STATSGO soil depths for the HRUs associated with the soil moisture measurement sites are: 1651 mm at site 057, 1016 mm at site 076, 584 mm at site 098, 483 mm at site 127 and 229 mm at site 176. For each of the sites, soil water storage was calculated at approximately similar depth as that of the associated HRU based on STATSGO soil classification.

Comparison of changes in soil water storage based on the observed and simulated soil moisture content is presented in Figure 7. Statistical comparison of the observed and modeled changes in soil water storage is presented in Table 8. Modeled changes in soil water storage showed a good correlation with the measured changes in soil water storage at all five soil water content measurement sites. The model predictions follow the seasonal patterns of soil water storage and matched the timing of peak soil water storage and summer dry spell quite well. The model performance statistics varies from NSE = 0.25 to 0.74, Pbias = 6.5% to -32.1%, R^2 = 0.59 – 0.80 and Slope = 0.81 to 1.13. Given the uncertainty associated with the measurements of soil moisture content and the scale difference between the measured (point measurements) and modeled (spatially average values for HRUs) soil water storage values, performance of the model in predicting the changes in soil water storage was reasonably good.

It is important to note that the observed and simulated change in soil water storage is presented in Figure 7 and statistics presented in Table 8 are computed for the STATSGO soil depths which are the shallowest at high elevation site (176) and deepest at lowest elevation site (057) as mentioned earlier. The Figure 7 indicates that the change in soil water storage is approximately in the similar range at all three soil moisture measurement sites. However, the change in soil water storage per unit depth of soil was greatest for the high elevation site (176) where the soils were shallowest. Similarly, the change in soil water storage per unit depth of soil was smallest at site 057 where the soils were deepest. The patterns in soil water storage per unit depth of soil were also in general agreement with the overall hydrologic characteristics of the watershed. High elevations, which receive more precipitation showed greater variability in soil water storage per unit depth while the low elevation sites which receive comparatively less precipitation showed smaller change in soil water storage per unit depth.

ii). Watershed Scale Hydroclimatology

The model predicted both streamflow and soil moisture storage changes over a wide range of elevation gradients in the watershed thus capturing the spatial variability in hydrologic processes across the watershed. These validation results facilitate in extending the prediction of the water balance components by the model to evaluate the watershed- scale hydrology across the range of elevations and vegetation cover.

a. Elevation impacts on Ecohydrological processes

In the mountain basins ecohydrologic conditions change rapidly with elevation. To understand the ecohydrological behavior across elevations of the RCEW, SWAT simulated water budget was analyzed for the three sub-basins. Drainage area for the RME, Tollgate and Outlet sub-basins are respectively 0.39 km^2, 55 km^2 and 238 km^2. Average annual precipitation is 1010 mm, 671 mm and 354 mm for the headwater RME, mid-elevation Tollgate and the RCEW watersheds, respectively.

Figure 8 (a-c) presents the simulated average monthly water budget for the RME, Tollgate and RCEW watersheds. At the high elevation RME watershed, orographic effects lead to higher precipitation, colder temperatures and greater snowfall fraction. Majority of precipitation falls as snow between November to March and about 80-95% of the total streamflow occur during the snowmelt period from March to June (Figure 8a). Streamflow patterns become progressively more uniform at mid-elevation (Tollgate) and Outlet gage locations as warmer conditions leads to an increase in the fraction of precipitation as rain (Figure 8b&c).

Other simulated water balance components also reflect the changing hydrologic regime with elevation. At RME, ET remains very low during winter (November-February) as plants become dormant due to cold climate conditions. In the spring, as snowpack begins to melt, both ET and soil water storage increases. Peak soil water storage occurs in May, nearly at the time of complete snowmelt. ET continues to rise in June when the ET demand is supplied by the soil water storage. Thereafter, both ET and soil water storage decrease due to limited water availability and hot and dry climate conditions. Soil water storage and ET rate reached at their minimum level near the end of the summer.

As conditions become progressively warmer towards lower elevations, plants become active earlier in the season. Hence, Tollgate and RCEW sub-basins show an increased soil water storage and ET earlier in the season and subsequently decrease to a minimum level earlier in the summer. At Tollgate peak soil water storage occurs in April while at RCEW peak soil water storage occurs in March. Similarly peak ET rate is few days early at Tollgate and about a month early at RCEW than at RME.

Figure 9 (a-c) shows the annual streamflow to precipitation (Q/P) ratio for both simulated and measured streamflow at the RME, Tollgate and Outlet gage locations. It is evident from Figure 9 that the Q/P ratio based on the simulated and observed streamflow matched best for the RME weir while at the Tollgate and Outlet weir Q/P ratio computed from simulated streamflow was higher than that of the observed streamflow-based Q/P. This pattern was expected as the model was overpredicting streamflow at the Tollgate and Outlet weirs. Overprediction of streamflow for both Tollgate and Outlet appeared to be greater for the low streamflow years while during the high streamflow years measured and predicted streamflow matched quite well (Figure 9b&c). Greater overprediction of Q/P ratio during the low streamflow years also implied that larger fraction of water was diverted for the agriculture during the dry water years.

At RME, most of the streamflow is generated by the spring snowmelt over a short period, resulting in smaller losses due to infiltration and ET and higher streamflow. At RME streamflow represents about 60% of the total annual precipitation (Figure 9a). In semi-arid environments ET normally is the second largest component, after precipitation, of the water budget but at RME, simulated ET was smaller than streamflow.

At lower elevations, conditions become progressively drier. This leads to an increase in ET fraction and a decrease in streamflow fraction of annual water budget. Precipitation and streamflow represent approximately an equal fraction of the annual water budget in the Tollgate subwatershed (Figure 8b & 9b). Whereas for RCEW watershed, drier conditions lead to greater ET fraction and smaller streamflow in the annual water budget (Figure 8c & 9c).

b. Hydroclimatic Variability due to vegetation

RCEW represents significant heterogeneity in vegetation. Location of the vegetation types are mainly driven by precipitation and climate conditions. Forest communities are mainly located at high elevation regions with colder climate conditions and higher precipitation. Figure 10 shows the differences in ET and precipitation from different vegetation classes of the RCEW.

Evergreen forests are located in regions with highest precipitation (764 mm) with greatest snow fraction (0.6). ET/P ratio is the lowest (0.5) in the evergreen forests due to cold climate and sufficient availability of water. Average annual precipitation in deciduous forests is 528 mm about half of which falls as snow with ET/P ratio of 0.57. Low and mid elevations of the watershed are primarily covered by mixed sagebrush, dry rangeland and agricultural grasslands. Long term average annual precipitation in the mixed sagebrush plant communities is 354 mm with snowfall fraction of about 0.34 and ET/P ratio of about 0.69. Vegetation classes of semi-arid rangeland and agricultural grasslands are primarily located in low to mid elevation regions and receive lowest precipitation (about 275mm), with warmest climate, lowest snowfall fraction (0.22) and greatest ET/P ratio (about 0.93).

It is clear from Figure 10 that the ET/P ratio is greatest for the semi-arid rangeland and agricultural grassland vegetation classes which receive the lowest precipitation and ET is primarily limited due to the availability of water. ET/P ratio decreases with an increase in precipitation as ET processes becomes less limited by the water availability. The forest vegetation classes which receive the most precipitation and are located in higher elevations and colder climate regions of the watershed have the lowest ET/P as sufficient water remain available for ET processes for most of the year.

3. Long-Term Hydroclimatology Assessment

a. Long-term water budget

Partitioning the water budget in RCEW is affected by both natural climate variability (wet-dry hydrologic cycles) as well as persistent warming climate conditions over the modeling period (1967-2006). Annual water budget for the sub-basins, RME, Tollgate and RCEW, for the modeling period are presented in Figure 11. This illustration presents the components of the water balance including total annual precipitation, measured and simulated streamflow, total ET, deep drainage and total change in soil water storage for each of the three sub-basins and it suggests the highly variable nature of hydrologic regime in the watershed.

The RME basin receives significantly higher precipitation than the rest of the watershed. Since the climate remain very cold throughout the winter and most of streamflow is generated due to spring snowmelt generated over a short period of time, ET is generally low and streamflow is generally the second largest component of the water budget. However, in dry years ET can be also be greater than streamflow as greater fraction of precipitation is required for soil moisture recharge and ET processes.

Total precipitation received by the Tollgate basin is less than that of the high elevation RME basin but greater than the overall precipitation collected in the entire watershed. Over the entire modeling period ET and streamflow represents approximately an equal fraction of the annual water budget. However, during the wet years streamflow is generally greater than ET as greater fraction of precipitation remain available after soil moisture recharge and ET. On the other hand, during the dry years streamflow can be significantly lower than ET as large fraction of precipitation is used for soil water recharge and ET.

The entire RCEW area represents typical semi-arid hydroclimatology with the water budget being dominated by precipitation and ET. Interestingly ET processes, especially at low to mid elevations of the RCEW, are mostly limited by the availability of soil moisture and most of the precipitation are used for soil water recharge and ET processes. Streamflow represents even a smaller fraction of the water budget and exhibits great variability between wet and dry years.

b. Wet-dry cycles

Hydrologic regime at RCEW goes through an alternate wet-dry cycles. As discussed in the previous section, both the water budget and streamflow generation during wet and dry years can vary greatly. Therefore, it is important to understand the hydrologic processes during both wet and dry hydrologic conditions. To demonstrate the variable nature of the hydrologic regime at RCEW, *Normalized Anomaly* (hereafter *Anomaly*) in the annual streamflow at three weirs were compared with the Palmer drought severity index (PDSI: Cook et al. 2004) (Figure 12). *Anomaly* is a measure of deviation from the long-term average conditions. *Anomaly* in the measured and modeled streamflow is computed using the following equation (Gruhier et al. 2008):

$$Normalized\ \ Anomaly = \frac{O - \overline{O}}{Std.Dev.} \quad (7)$$

where O is the observed annual streamflow, Ō is the long-term mean annual streamflow. Here positive values of *anomaly* indicate greater than the average streamflow and negative values of *anomaly* indicate less than the average streamflow.

PDSI for RCEW is estimated as an average of four PDSI grid points (Cook et al. 2004; published at http://www.ncdc.noaa.gov/paleo/newpdsi.html) adjacent to RCEW. PDSI index is a measure of hydrologic variability and varies between -6 to +6. Similar to the *Anomaly* concept, positive PDSI index values indicate wetter than normal and negative PDSI index values indicate drier than normal conditions. A year with a PDSI value of 4 or greater is considered as an extremely wet year while a year with a PDSI value or -4 or less is considered as an extremely dry year.

Figure 12 presents the comparison of *anomaly* in the measured and simulated streamflow with the PDSI index for the RCEW. At all three weirs, *anomaly* index computed using both measured (Figure 12a) and simulated (Figure 12b) streamflow follows similar trends which indicate that the model was able to capture the natural variability in hydrologic conditions due to wet-dry cycles. It is evident from Figure 12 that hydrologic regime at the RCEW follows the wet and dry periods of PDSI and is highly variable. Hydrologic regime at RCEW, like rest of the intermountain west, is strongly affected by the El-Nino southern oscillation (ENSO) and goes through a period of 3 to 7 years of wet and dry spells. Understanding of streamflow patterns in the mountainous regions during the periods of wet-dry spells is important for water management purposes. Storage reservoirs are filled during the wet spells to meet the water deficit during the drought cycles.

It is important to understand the hydrologic processes during both wet and dry periods to better understand hydrologic behavior of the RCEW. Basin average monthly water balance during a wet (1984) and a dry (1987) water year is presented in Figure 13. In the wet year, 1984, peak stream discharge occurred in May, about a month earlier than the dry 1987 water year. Peak soil water storage in 1987 was simulated in March which is also about a month earlier than that of the wet water year, i.e 1984.

During 1984 water year, peak ET was simulated in May, thereafter both ET and soil water storage declined due to warm and dry climate conditions and limited soil water availability for plants. Whereas in 1987, peak ET was simulated in June because of summer precipitation events in late May and early June. For the dry year both soil water storage and ET rates remained lower than normal and by the end of the water year ET became negligible and soil water storage reached its lowest level.

Monthly spatial distribution of ET and soil water storage during the growing seasons of the wet 1984 and dry 1987 are presented in Figure 14 and 15, respectively to demonstrate the differences in ecohydrological processes during wet and dry years. In Figure 15, measured soil water storage at five measurement sites is superimposed on the simulated soil moisture plot. Visual inspection of this illustration clearly shows that the modeled soil water storage matches well with the measured soil water storage and were able to capture both spatial and temporal variability in soil moisture during both wet (1984) and dry (1987) water years. Spatial distribution of soil water storage shows that the soil moisture level across high elevations and western slopes remain relatively higher than the rest of the watershed throughout the growing season during both wet and dry water years. Orographic and wind effects lead to more precipitation over high elevations and the western slopes of RCEW, these spatial patterns in soil water storage indicate that the model is adequately distributing the precipitation patterns over the watershed.

Spatial distribution of soil water storage and ET during 1984, wet water year, shows that during March ET remain negligible in most of the watershed except for a few low elevation regions even though significant water was present as soil water storage due to very cold climate conditions and snow cover. In April, soil water storage increased as the snowpack began to melt away, plants became active over most of the watershed except a few high elevation regions where snow cover persisted till late spring. By May and June, plants became active in the entire watershed and ET rates were near their peaks with a range of values as low as 25-50 mm in low elevations to as high as 150-200 mm in high elevations. Low elevation soil profile started drying down due to plant water extraction while soil water storage at mid to high elevations remained relatively high due to snowmelt from high elevations. In July, as soil water storage continued to deplete ET rates became very low (<10 mm) at few low elevation regions while ET rates remained substantially higher (between 25 to 150 mm) across mid to high elevations. As summer progressed,

soils became very dry and the areas with very low soil water storage (<10 mm) and ET rates (<10 mm) grew. Still a few high elevation regions, mostly covered by forest communities, where the soil column remained relatively moist (10-100 mm) and ET remained substantially high (between 10-50 mm) till the end of the water year.

The 1987 water year was a warm and dry water year. Snow cover melted away from most of the low to mid elevations of the watershed by March. Plant communities existed over low to mid elevations of the watershed were greening up (ET rates between 25-75 mm) while at high elevations ET (between 10-25 mm) was still negligible due to snow cover and cold conditions. By April, almost entire watershed was snow free and plants at the higher elevations also engaged in the ET process. ET rates from few of the low elevation areas were very low due to soil moisture stress. A spring rain storm during late May and early June led to increased soil water availability and increased ET rates. Thereafter dry summer followed and soils started drying down below the wilting point and plants senesced, ET ceased. There was no ET from most of the low elevation regions by July. Areas with very dry soils and negligible ET grew with the hot and dry summer. By the end of water year soil water storage in the entire watershed was less than 10 mm and ET rates were negligible.

c. Trends in the timing of streamflow

To analyze how warming climate conditions have changed the hydrologic cycle of RCEW, we analyzed streamflows for changes in the timing of peak flow and overall seasonal (annual or monthly) variations. Warming climate conditions are expected to cause early snowmelt and streamflow over the interior west. We used the Center of Timing (CT) concept to evaluate the changes in the seasonal patterns of streamflow for both the measured and simulated streamflow data from RME, Tollgate and Outlet weirs. CT is defined as the timing of the center of mass of total water year streamflow (Stewart et al. 2004; Cayan et al. 2001) and calculated at follows:

$$CT = \frac{\sum t_i q_i}{\sum q_i} \qquad \text{----------(8)}$$

where t_i is the time in months (or days) from the beginning of the water year and q_i is the corresponding streamflow for month (or day). CT has been previously used to report changes in streamflow timings of the snowmelt dominated rivers of the Northwest. (Stewart et al. 2004; Cayan et al. 2001). The trends in CT for both observed and simulated streamflow for all three weirs are presented in Figure 16.

Mean timing of CT dates were May 2 for measured streamflow and May 1 for simulated streamflow at RME. As contribution of rain and in turn the total streamflow increased near the downstream weirs, CT occurred progressively earlier. However, our analysis show that CT at Tollgate occurred about 15-20 days earlier than that of the RME weir and the mean CT days were April 18 and April 14 for the measured and simulated streamflow, respectively. At Outlet the occurrence of CT was further advanced and the mean dates of CT were April 5 and April 10 for the measured and simulated streamflow, respectively. Gradual advancement of mean CT from upstream to downstream weirs clearly indicate the change in the watershed behavior impacted variably between the snowmelt-dominated headwater catchment and rain-dominated downstream regions of the watershed.

Measured streamflow at RME showed a trend towards earlier CT by approximately 8 days and the simulated streamflow showed a trend towards earlier CT by approximately 10 days over the simulation period (1967-2006). However, Tollgate and Outlet gages showed opposite trends in CT for the simulated and measured streamflow. Streamflows at Tollgate indicate an earlier CT by about 7 days for the simulated streamflow and delayed CT by about 5 days for the measured streamflow over the simulation period (1967-2006). Analysis for the Outlet weir showed an earlier CT by about 10 days for the simulated streamflow and a lag of about 28 days for measured streamflow over the simulation period (1967-2006).

Simulation results indicated the trends towards earlier streamflow timings at all three weirs of RCEW. Measured streamflow data only indicated earlier streamflow timings at RME while Tollgate and Outlet showed trends toward later streamflow timings. Many studies have reported the earlier streamflow timings from the snowmelt-dominated basins due to warmer climate conditions (Cayan et al. 2001; Stewart et al. 2004, 2005; Regonda et al. 2005). The CT trends in simulated streamflow at all three weirs and measured streamflow at the RME weir were in agreement with these studies. It is important to note that streamflow at Tollgate and Outlet are partially affected by the unaccounted withdrawal of water for agriculture. Since the agricultural withdrawal of water begins in March-April, it tended to

delay the CT timings. Therefore, the CT trends at RME weir derived from the simulated streamflow probably better represent the effects of warming climate conditions in the computation of streamflow timing.

Earlier timing of streamflow can have serious implications on local and regional ecosystems. Local vegetation depends on streamflow during late spring and summer to meet their water demand during the drier part of the year. Earlier timing of peak streamflow would mean lower streamflow during late spring and summer when soils are driest causing water stress to vegetation. Regional water management strategies are also based on the storage of water from snowmelt to fulfill water demand for agricultural, domestic, industrial and environmental purposes. Adjustment in the water management strategies would be necessary to adopt for the changes in the timing of streamflow.

5. Conclusion

SWAT model was carefully calibrated to simulate hydrology of the RCEW, a snowmelt dominated semi-arid mountain basin. Mountain basins exhibit tremendous spatial variability and relative importance of hydrologic processes changes rapidly. Processes and parameters governing different climate regions within the watershed were identified. Model was calibrated separately at high elevation, mid elevation and low elevation weirs which enabled accurate parameterization at high, mid and low elevation regions of the watershed. The model predicted both total volumes and seasonal patterns in streamflow for all the three long-term weirs. Simulation results also showed good agreement with the measured soil water storage.

Mountain basins exhibit great spatial variability. Capturing the spatial variability in hydro-climatic processes is essential for accurate hydrologic predictions in these mountain basins. The results of this study demonstrated that the SWAT model can be successfully used to simulate hydrologic processes in the complex mountain basins. However, careful distribution of forcing climate data, identification of governing hydrologic processes and sensitive model parameters However, it is essential to accurately distribute forcing climate data based on understanding of physical processes over the watershed. Careful identification of the governing hydrological processes and calibration of parameters is also required to characterize the hydrological response in each of the hydroclimatic zones within the watershed.

Model simulation results were analyzed for each sub-basin and land use class to demonstrate the heterogeneous nature of the hydrologic regime in RCEW. Model predictions indicated that at high elevations where snowmelt processes were dominant and precipitation was high, Q/P ratio was the highest and ET/P ratio was the lowest as compared to the rest of the watershed. Q/P ratio progressively decreased and ET/P ratio increased towards lower elevations as precipitation became progressively more limited.

ET/P ratio was greatest for the dry rangeland and agricultural grasslands, located in the driest valley region of the watershed and lowest for the forest communities primarily located in the wettest-high elevation regions of the watershed. Analysis of simulated streamflow predictions showed trends towards earlier CT timings which indicated advances in snowmelt and streamflow timings.

Results of this research indicate that the SWAT model can be used for simulation of hydrologic processes in the snowmelt dominated semi-arid mountain basins. Findings of this research will be helpful in understanding the hydrologic behavior of the complex mountain basins of the intermountain west. This research will also be helpful in understanding the impacts of warming climate conditions related to shifts in the hydrologic regime in these semi-arid mountain basins.

References

Arnold, J.G., Srinivasan, R., Muttiah, R.S., Williams, J.R., 1998. Large area hydrologic modeling and assessment part I: model development. *Journal of American Water Resources Association* 35, 1037-1052.

Cayan D. R., Redmond, K.T., Riddle, L. G., 1999. ENSO and Hydrologic Extremes in the Western United States. *Journal of Climate* 12, 2881-2893.

Cayan D. R., Kammerdiener, S.A., Dettinger, M.D., Caprio, J.M., Peterson, D.H., 2001. Changes in the onset of spring in the western United States. *Bulletin of American Meteorological Society* 82, 399-416.

Cook, E.R., Woodhouse, C.A., Eakin, C.M., Meko, D.M., Stahle, D.W., 2004. Long-Term Aridity Changes in the Western United States. *Science* 306, 1015 – 1018.

Cooley, K.R., Hanson, C.L., Johnson, C.W., 1988. Precipitation erosivity index estimates in cold climates. *Transactions of ASAE* 31, 1445-1450.

Criss, R.E., Winston, W.E., 2008. Do Nash values have value? Discussion and alternate proposals. *Hydrological Processes* 22, 2723-2725.

Demirel, M.C., Venancio, A., Kahya, E., Flow forecast by SWAT model and ANN in Pracana basin, Portugal. *Advances in Engineering Software* 40 (7), DOI: 10.1016/j.advengsoft.2008.08.002, 467-473.

Duan, Q., Gupta, V.K., Sorooshian, S., 1992. Effective and efficient global optimization for conceptual rainfall-runoff models. *Water Resources Research* 28, 1015-1031.

Flerchinger, G.N., Cooley, K.R., 2000. A ten-year water balance of a mountainous semi-arid watershed. *Journal of Hydrology* 237, 86-99.

Flerchinger, G.N., Marks, D., Hardegree, S.P., Nayak, A., Winstral, A.H., Seyfried, M.S., Pierson, F.P., Clark, P.E., 2007. 45 years of climate and hydrologic research conducted at the Reynolds Creek Experimental Watershed. pp. 135-143 in: *J.R.Rogers ed), Environmental And Water Resources: Milestones In Engineering History.* Sponsored by ASCE Environmental and Water Resources Institute EWRI) National History & Heritage Committee. American Society of Civil Engineers, Reston, VA. 168 p.

Flerchinger, G.N., Cooley, K.R., Hanson, C.L. Seyfried, M.S., 1998. A uniform versus an aggregated water balance of a semi-arid watershed. *Hydrological Processes* 12**,** 331–342.

Fontaine, T.A., Cruickshank, T.S., Arnold, J.G., Hotchkiss, R.H., 2002. Development of a snowfall-snowmelt routine for mountainous terrain for the Soil and Water Assessment Tool (SWAT). *Journal of Hydrology* 262**,** 209-223.

Green, W. H., Ampt, G.A., 1911. Studies on soil physics, 1: The flow of air and water through soils. *Journal of Agricultural Science* 4, 1–24.

Gruhier, C., de Rosnay, P., Kerr, Y., Mougin, E., Ceschia, E., Calvet, J.-C., 2008. Evaluation of AMSR-E soil moisture product based on ground measurements over temperate and semi-arid regions. *Geophysical Research Letters*, 35, doi:10.1029/2008GL033330, 2008

Gui, G.O., Rosbjerg, D., 2009. Modelling of hydrologic processes and potential response to climate change through the use of a multisite SWAT. *Water and Environment Journal*, 10.1111/j.1747-6593.2008.00146.x, 1-11.

Hamlet, A. F., Mote, P.W., Clark, M.P., Lettenmaier, D.P., 2005. Effects of temperature and precipitation variability on snowpack trends in the Western United States. *Journal of Climate* 18, 4545-4561.

Hamon, W.R., 1971. Reynolds Creek, Idaho(Chapter 4). *Agricultural Research Service Precipitation Facilities and Related Studies. D. M. Hershfield eds.,* ARS-USDA, Washington, D.C., 25-35.

Hamon, W.R., 1973. Computing actual precipitation: Distribution of precipitation in mountainous areas. *WMO Rep. No. 362,* World Meteorological Organization, Geneva, 1, 159-173.

Hanson, C.L., 2001. Long-term precipitation database, Reynolds Creek Experimental Watershed, Idaho, United States. *Water Resources Research* 37, 2831-2834.

Hanson, C.L., Marks, D., Van Vactor, S. S., 2001. Long-term climate database, Reynolds Creek Experimental Watershed, Idaho, United States. *Water Resources Research* 37, 2839-2841.

Hanson, C.L., Pierson, F.B., Johnson, G.L., 2004. Dual-gauge system for measuring precipitation: historical development and use. *Journal of Hydrological Engineering* 9, 350-359.

Hanson, C.L., Johnson, G. L., Rango, A., 1999. Comparison of precipitation catch between nine measuring systems. *Journal of Hydrological Engineering* 4, 70-75.

Hanson, C.L., 1982. Distribution and stochastic generation of annual and monthly precipitation on a mountainous watershed in southwest Idaho. *Water Resources Bulletin* 18, 875-883.

Hargreaves, G.H. Samani, Z.A., 1985. Reference crop evapotranspiration from temperature. Transactions of ASAE, 1, 96-99.

Lemonds, P J., McCray, J. E., 2007. Modeling hydrology in a small rocky mountain watershed serving large urban populations. *Journal of American Water Resources Association* 43, 875-887.

Luce, C.H., Tarboton, D.G., Cooley, K.R., 1998. The influence of the spatial distribution of snow on basin-averaged snowmelt. *Hydrological Processes* 12, 1671-1683.

Marks, D., Winstral, A., Seyfried, M., 2002. Simulation of terrain and forest shelter effects on patterns of snow deposition, snowmelt and runoff over a semi-arid mountain catchment. *Hydrological Processes* 16, 3605-3626.

Marks, D., Winstral, A., 2001. Comparison of snow deposition, the snow cover energy balance, and snowmelt at two sites in a semiarid mountain basin. *Journal of Hydrometeorology* 2, 213-227.

Marks, D., King, G.A., Jayne, D., 1993. Implications of climate change for the water balance of the Columbia River Basin, USA. *Climate Research* 2, 203-213.

Marks, D., Domingo, J., Susong, D., Link, T., Garen, D., 1999. A spatially distributed energy balance snowmelt model for application in mountain basins. *Hydrological Processes* 13, 1935-1959.

Marks, D., Cooley, K.R., Robertson, D.C., Winstral, A., 2001. Long-term snow database, Reynolds Creek Experimental Watershed, Idaho, United States. *Water Resources Research* 37, 2835-2838.

Monteith, J. L., 1965. Evaporation and environment. *Symp. Soc. expl. Biol* , 19, 205-234.

Mote, P. W., 2003. Trends in snow water equivalent in the Pacific Northwest and their climatic causes. *Geophysical Research Letters* 30, 1601, doi:10.1029/2003GL017258, 2003.

Mote, P. W., 2006. Climate-driven variability and trends in mountain snowpack in Western North America. *Journal of Climate* 19, 6209-6220.

Mote, P. W., Hamlet, A.F., Clark, M.P., Lettenmaier, D.P., 2005. Declining mountain snowpack in Western North America. *Bulletin of American Meteorological Society* 86, 39-49.

Nash, J.E., Sutcliffe, J.V., 1970. River flow forecasting through conceptual models, part I: A discussion of principles. *Journal of Hydrology* 10, 282-290.

Nayak, A., Chandler, D.G., Marks, D., McNamara, J.P., Seyfried, M., 2008b. Correction of electronic record for weighing bucket precipitation gauge measurements, *Water Resources Research* 44, W00D11, doi:10.1029/2008WR006875.

Nayak, A., Marks, D., Chandler, D.G., Seyfried, M., 2008a. Long-term Snow, Climate and Streamflow Trends from at the Reynolds Creek Experimental Watershed, Owyhee Mountains, Idaho, USA., *Water Resources Research* (In review).

Neitsch, S.L., Arnold, J.G., Kiniry, J.R., Williams, J.R., 2005. Soil and water assessment tool: Theoretical documentation: Version 2005. Texas: USDA-ARS GSWRL and Blackland Research Center, Texas Agricultural Experiment Station.

Olivera, F., Valenzuela, M., Srinivasan, R., Choi, J., Cho, H., Srikanth, K., Agrawal, A., 2006. ArcGIS-SWAT: A geodatabase model and GIS interface for SWAT. *Journal of American Water Resources Association* 42, 295-309.

Penman, H. L. 1956: Evaporation: an introductory survey. *Neth. J. Agr. Sci.* , 4, 9-29.

Peschel, J. M., Haan, P.K., Lacey, R.E., 2006. Influences of soil dataset resolution on hydrologic modeling. *Journal of American Water Resources Association* 42, 1371-1389.

Priestley, C.H.B., Taylor, R.J., 1972. On the assessment of surface heat flux and evaporation using large-scale parameters. *Monthly Weather Review* 100, 81-82.

Regonda, S. K., Rajagopalan, B., Clark, M., Pitlick, J., 2005. Seasonal cycle shifts in hydroclimatology over the Western United States. *Journal of Climate* 18, 372-384.

Robins, J. S., Kelly, L. L., Hamon, W.R., 1965. Reynolds Creek in southwest Idaho: an outdoor hydrologic laboratory. *Water Resources Research* 1, 407-413.

Seyfried, M. S., Murdock, M.D., Hanson, C.L., Flerchinger, G.N., Van Vactor, S., 2001. Long-term soil water content database, Reynolds Creek Experimental Watershed, Idaho, United States. *Water Resources Research* 37, 2847-2851.

Slaughter, C.W., Marks, D., Flerchinger, G.N., Van Vactor, S.S., Burgess, M.D., 2001. Thirty-five years of research data collection at Reynolds Creek Experimental Watershed, Idaho, United States. *Water Resources Research* 37, 2819-2823.

Stewart, I. T., Cayan, D.R., Dettinger, M.D., 2004. Changes in snowmelt runoff timing in Western North America under a 'Business As Usual' Climate Change scenario. *Climatic Change* 62**,** 217-232.

Stewart, I. T., Cayan, D.R., Dettinger, M.D., 2005. Changes towards earlier streamflow timing across Western North America. *Journal of Climate* 18, 1136-1155.

Stratton, B. T., Sridhar, V., Gribb, M.M., McNamara, J.P., Narasimhan, B., 2009. Modeling the spatially varying water balance processes in a semi-arid mountainous watershed of Idaho. *Journal of American Water Resources Association* (in press).

Tarboton D. G., Luce, C.H., 1996. Utah Energy Balance snow accumulation and melt model UEB). Computer model technical description and users guide. *Utah Water Research Laboratory, Utah State University and USDA Forest Service Intermountain Research Station.*

Trenberth, K. E., Jones, P.D., Ambenje, P., Bojariu, R., Easterling, D., Tank, A.K., Parker, D., Rahimzadeh, F., Renwick, J.A., Rusticucci, M., Soden, B., Zhai, P., 2007. Observations: Surface and atmospheric climate change. *Climate change 2007: The physical science basis.* Contributions of Working Group I to the Fourth Assessment Report of the Intergovernmental Panel on Climate Change, S. Solomon, D. Quin, M. Manning, Z. Chen, M. Marquis, K. B. Averyt, M. Tignor, and H. L. Miller, eds., Cambridge University Press, Cambridge, UK and New York, 235-336.

USDA-SCS, 1972: *National Engineering Handbook* Section 4, Hydrology. USDA-SCS, Washington, DC, USA.

Van Griensven, A., Meixner, T., Grunwald, V., Bishop, V., Diluzio, M., Srinivasan, R., 2006. A global sensitivity analysis tool for the parameters of multi-variable catchment models. *Journal of Hydrology* 324, 10-23.

Van Liew, M.W., Veith, T.L., Bosch, D.D., Arnold, J.G., 2007. Suitability of SWAT for the conservation effects assessment project: comparison on USDA Agricultural Research Service watersheds. *Journal of Hydrological Engineering* 12, 173-189.

Wang, X., Melesse, A.M., 2006. Effects of STATSGO and SSURGO as inputs on SWAT models snowmelt simulation. *Journal of American Water Resources Association* 42, 1217-1236.

Williams, J. R., 1969. Flood routing with variable travel time or variable storage coefficients. Transactions of ASAE 12, 100-103.

Winstral, A., Marks, D., 2002. Simulating wind fields and snow redistribution using terrain-based parameters to model snow accumulation and melt over a semi-arid mountain catchment. *Hydrological Processes* 16, 3585-3603.

Winstral, A., Elder, K., Davis, B., 2002. Modeling the effects of wind induced snow redistribution with terrain-based parameters to enhance spatial snow modeling. *Journal of Hydrometeorology* 3, 524-528.

Zhang, X., Srinivasan, R., Debele, B., Hao, F., 2008. Runoff simulation of the headwaters of the yellow river using the swat model with three snowmelt algorithms. *Journal of American Water Resources Association* 44, 48-61.

Table Captions

Table 1: Precipitation, Meteorological and Soil Moisture data.
Table 2: Streamflow gaging station location and details of data.
Table 3: Snowmelt parameters selected for calibration of the watershed.
Table 4: Calibrated model parameters for the RME sub-basin.
Table 5: Calibrated model parameters for the Tollgate weir sub-basin.
Table 6: Calibrated model parameters for the Outlet weir sub-basin.
Table 7: Statistical analysis of streamflow prediction at the RCEW.
Table 8: Site-wise comparison of measured and modeled soil water storage across the watershed.

Figure Captions

Figure 1: DEM map of the RCEW showing locations of precipitation gauges, climate stations, soil moisture stations and weirs.
Figure 2: Long-term monthly average streamflow at (a) RME weir, (b) Tollgate weir and (c) Outlet weir.
Figure 3: Land use cover map of the RCEW showing five types of land cover classes.
Figure 4: STATSGO soils map of the RCEW.
Figure 5: (a) Temperature lapse rate and (b) Precipitation lapse rate at RCEW.
Figure 6: Comparison of observed and simulated streamflow for the three long term weirs during (a) Calibration phase (1997-2006) and (b) Validation phase (1967-1996).
(c) Representation of parameter calibration estimation using autocalibration function in SWAT with the objective function of sum of the square of the residuals (SSQ).

Figure 7: Comparison of measured and modeled soil water storage change at five soil moisture measurement sites and the HRUs in which they are located.
Figure 8: Average monthly water budget at (a) RME, (b) Tollgate and (c) RCEW basins, showing precipitation, evapotranspiration, soil water storage, percolation and simulated and measured streamflow.
Figure 9: Comparisons of Annual Streamflow-Precipitation (Q/P) ratio for simulated and measured streamflow at (a) RME (b) Tollgate and (c) Outlet weirs.
Figure 10: Evapotranspiration to precipitation (ET/P) ratio and snow fraction at each of the land use types of the RCEW. Average precipitation depth in each land cover class is shown as the numbers in the bars.
Figure 11: Annual water budget at (a) RME (b) Tollgate and (c) RCEW basins showing annual precipitation, evapotranspiration, annual change in soil water storage, deep drainage and simulated and measured streamflow.
Figure 12: Palmer Drought Severity Index for RCEW and Normalized Anomaly at RME, Tollgate and Outlet weirs for (a) measured streamflow and (b) simulated streamflow.
Figure 13: Monthly distribution of the water balance components during (a) wet (1984) and (b) dry water years.
Figure 14: Simulated monthly ET distributions during wet (1984) and dry (1987) water years.
Figure 15: Simulated monthly soil water storage distributions during wet (1984) and dry (1987) water years.
Figure 16: Simulated and Measured CT plots for the Outlet, Tollgate and RME weirs in RCEW.

Table 1: Precipitation, Meteorological and Soil Moisture data.

Site ID	Name	Easting	Northing	Elevation	Data Type	Period of Records
057	Flats	521408	4786027	1184	P	1/1/1962-12/31/2006
					SM	1971-2006
076	Quanset	520334	4783383	1203	P	1/1/1962-12/31/2006
					Tmax &Tmin	1/1/1964-12/31/2006
					SM	1981-2006
098	Nancy Gulch	523352	4779402	1414	P	3/17/1972-12/31/2006
					SM	1971-2006
116		519000	4776346	1460	P	1/1/1962-12/31/2006
127	Lower Sheep Creek	521759	4776190	1650	P	1/1/1962-12/31/2006
					Tmax &Tmin	1/1/1967-12/31/2006
					SM	1972-2006
138		522588	4774248	1868	P	10/8/1983-12/31/2006
144		515952	4771978	1815	P	1/1/1962-12/31/2006
147		521334	4772332	1872	P	1/1/1962-12/31/2006
155		518421	4771319	1653	P	1/1/1962-12/31/2006
163		514140	4769423	2169	P	1/1/1962-12/31/2006
167		521595	4769781	2001	P	1/1/1962-12/31/2006
174		516822	4768029	2073	P	1/1/1962-12/31/2006
176	Reynolds Mtn.	519693	4767898	2094	P	1/1/1968-12/31/2006
					Tmax &Tmin	1/1/1967-12/31/2006
					SM	1973-2006
rmsp	Reynolds Mtn. Snow Pillow	520054	4768116	2056	P	1/1/1962-12/31/2006

* P = Precipitation; Tmax & Tmin = Daily Maximum and Minimum Temperature; SM = Soil Moisture
** Easting, Northing and Elevation in meters; NAD83 Zone 11 projections

Table 2: Streamflow gaging station location and details of data.

Gauge ID	Name	Easting (m)	Northing (m)	Elevation Range (m)	Drainage Area (km^2)	Period of Records
166	Reynolds Mtn. East	519954	4768494	2024-2139	0.39	1/1/1963-12/31/2006
116	Tollgate	519393	4776495	1398-2244	54.68	3/29/1966-12/31/2006
036	Outlet	520111	4789673	1099-2244	238.22	1/1/1963-12/31/2006

Easting, Northing and Elevation in meters; NAD83 Zone 11 projections
Drainage Area in km^2

Table 3: Snowmelt parameters selected for calibration of the watershed.

Parameter	Description	Lower Bound	Upper Bound	Optimized Value	Reference
SMFMX	Maximum melt rate on June 21 (mm/°C/Day)	0	10	6.5	Fontaine et al. (2002)
SMFMN	Minimum melt rate on December 21 (mm/°C/Day)	0	10	4.0	Fontaine et al. (2002)
SNOCOVMX	Areal snow coverage threshold at 100% snowcover (mm)	0	650	300	Fontaine et al. (2002)
SNO50COV	Fraction of SNOCOVMX that provides 50% snowcover	0	1	0.5	Fontaine et al. (2002)
SFTMP	Snowfall base temperature (°C)	-5.0	5.0	1.0	
SMTMP	Snowmelt threshold temperature (°C)	-5.0	5.0	2.0	
TIMP*	Snowpack temperature lag factor	0.01	1.0	0.185	

* Calibrated using automated SCE algorithm.

Table 4: Calibrated model parameters for the RME sub-basin.

Parameter	Description	Lower Bound	Upper Bound	Optimized Value
ALPHA_BF	Baseflow alpha factor (days)	0	1	0.7
GWQMN	Threshold depth of water in shallow aquifer for base flow to occur (mm)	0	5000	109.1
RCHRG_DP	Deep recharge fraction	0.1	1	0.822
REVAPMN	Threshold depth of water in shallow aquifer for revaporation to occur (mm)	0	500	231.728
SLOPE	Average slope steepness (m/m)	-10%	+10%	7.39 %

Table 5: Calibrated model parameters for the Tollgate weir sub-basin.

Parameter	Description	Lower Bound	Upper Bound	Optimized Value
CN2	Curve number for the Antecedent moisture condition 2	-10%	10%	-10%
ESCO	Soil evaporation compensation factor	0.8	1.0	0.9
GWQMN	Threshold depth of water in shallow aquifer for base flow to occur (mm)	0	500	36.036
RCHRG_DP	Deep recharge fraction	0.6	0.85	0.695
REVAPMN	Threshold depth of water in shallow aquifer for revaporation to occur (mm)	0	100	20.466
SLOPE	Average slope steepness (m/m)	-10%	+10%	-9.89%

Table 6: Calibrated model parameters for the Outlet weir sub-basin.

Parameter	Description	Lower Bound	Upper Bound	Optimized Value
CN2	Curve number for the Antecedent moisture condition 2	-10%	10%	-9.98%
ESCO	Soil evaporation compensation factor	0.8	1.0	0.8
GWQMN	Threshold depth of water in shallow aquifer for base flow to occur (mm)	0	500	2.237
RCHRG_DP	Deep recharge fraction	0.6	0.9	0.850
SLOPE	Average slope steepness (m/m)	-10%	+10%	-10%
SOL_AWC	Available soil water capacity	-10%	+10%	10%

Table 7: Statistical analysis of streamflow prediction at the RCEW.

Weir Name	Period	Simulation Type	NSE	Pbias	RMSE	R^2	Slope
RME	1967-1996	Val.	0.89	5.17	0.004	0.89	0.89
	1997-2006	Cal.	0.90	7.69	0.004	0.90	0.96
Tollgate	1967-1996	Val.	0.82	-12.67	0.283	0.85	1.00
	1997-2006	Cal.	0.84	-9.44	0.247	0.87	1.02
Outlet	1967-1996	Val.	0.68	-10.87	0.481	0.71	0.85
	1997-2006	Cal.	0.70	-26.67	0.394	0.82	1.08

Table 8: Site-wise comparison of measured and modeled soil water storage across the watershed.

Soil Moisture Site	Soil Depth (mm)	Period	NSE	Pbias (%)	RMSE	R^2	Slope
057	1651	Jan 1976- Dec 2006	0.58	6.5	0.82	0.68	0.94
076	1016	Jan 1981- Nov 1995	0.25	-6.9	0.63	0.80	1.13
098	584	Jan 1976- Nov 1995	0.35	-22.7	0.77	0.59	0.92
127	483	Feb 1976- Nov 1995	0.74	-4.2	0.87	0.76	0.88
176	229	Apr 1977- Dec 2006	0.50	-32.1	0.82	0.67	0.81

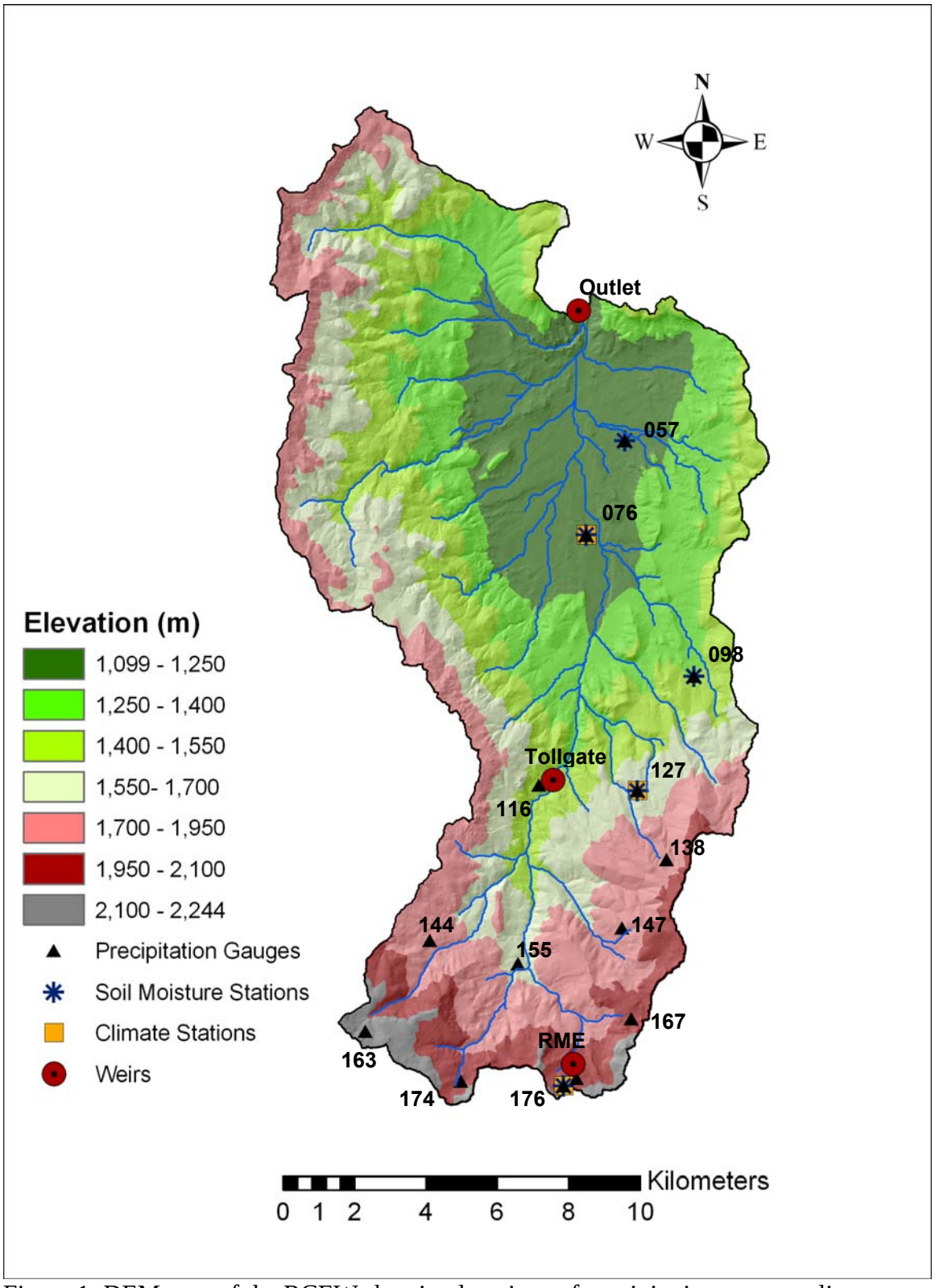

Figure 1: DEM map of the RCEW showing locations of precipitation gauges, climate stations, soil moisture stations and weirs.

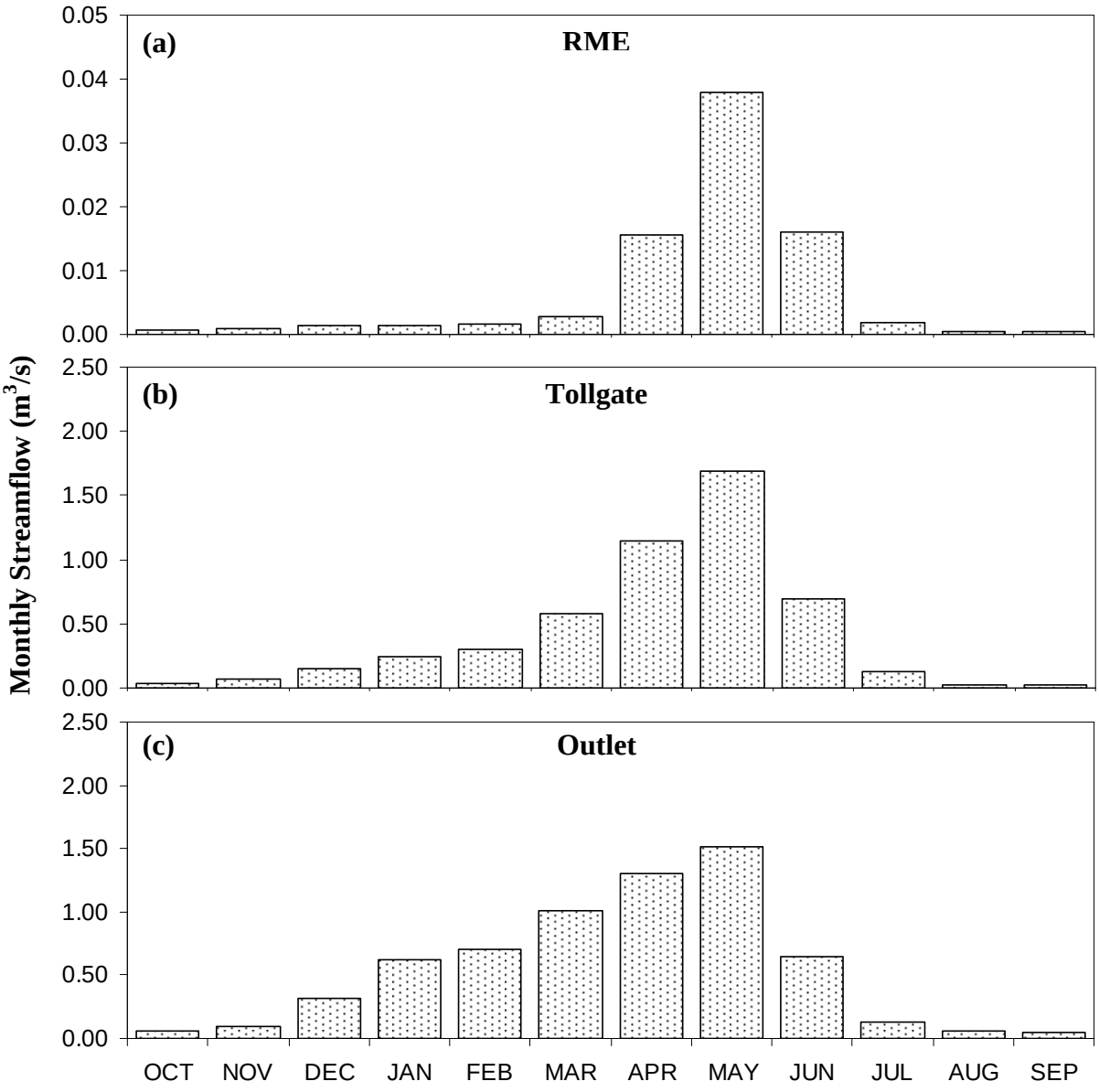

Figure 2: Long-term monthly average streamflow at (a) RME weir, (b) Tollgate weir and (c) Outlet weir.

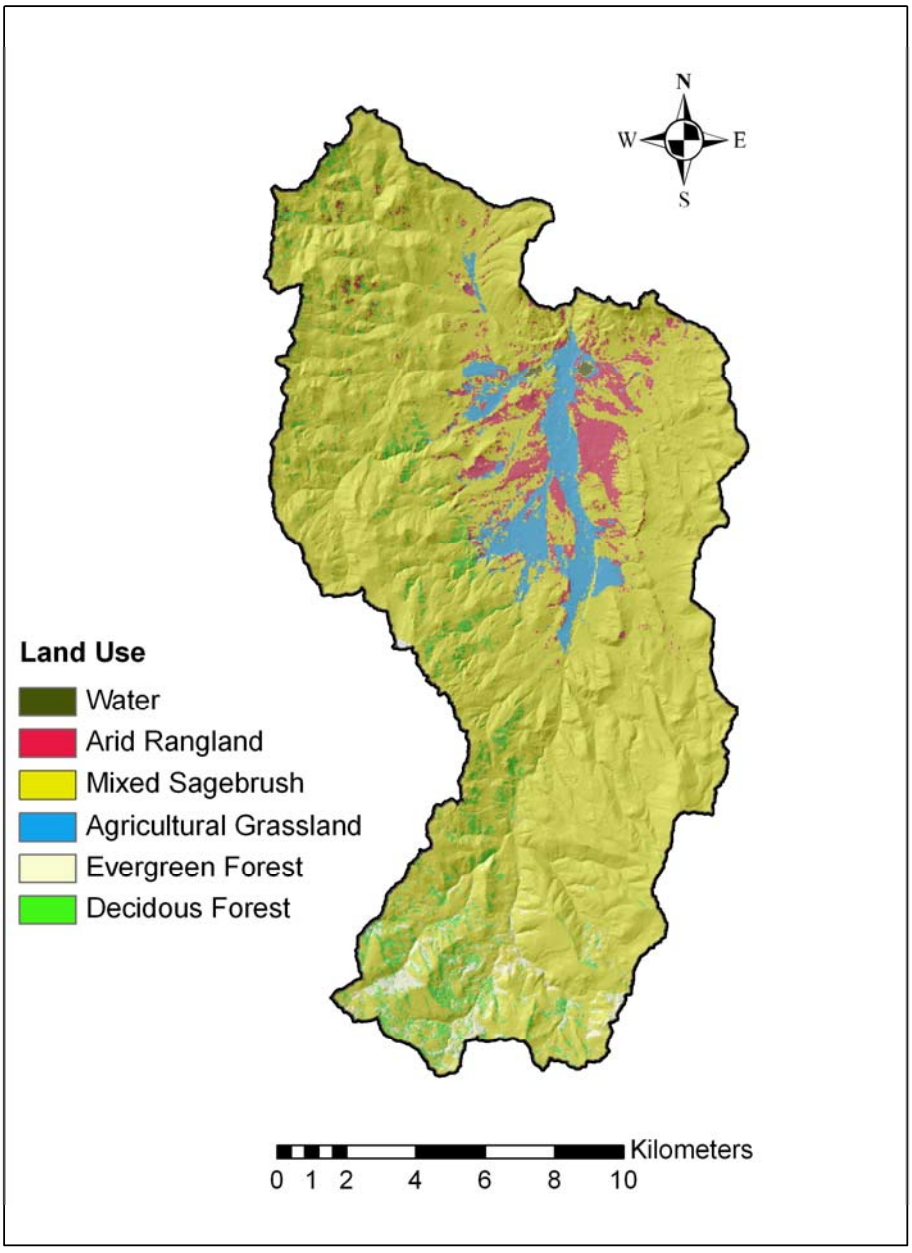

Figure 3: Land cover map of the RCEW showing five types of land cover classes.

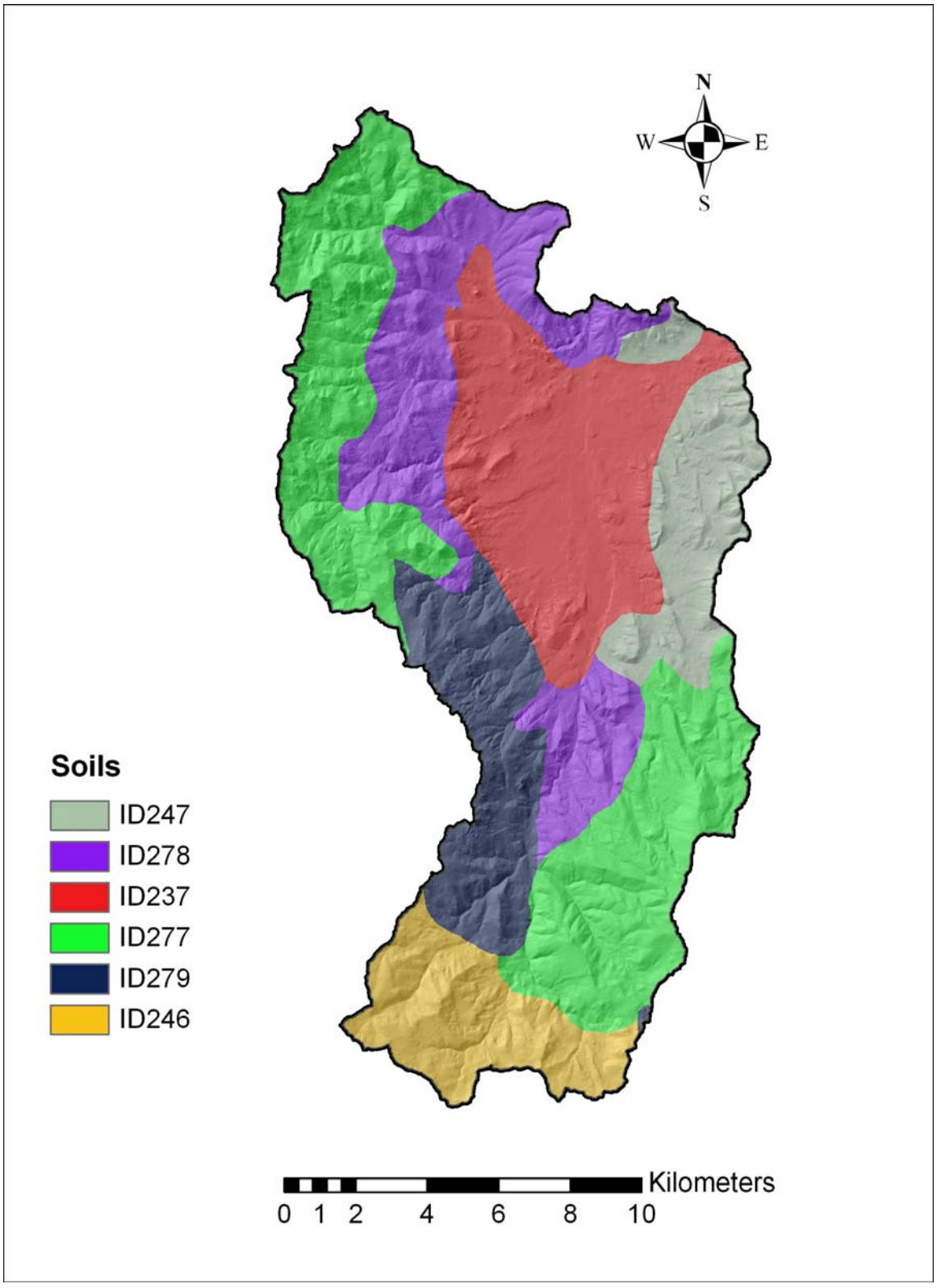

Figure 4: STATSGO soils map of the RCEW.

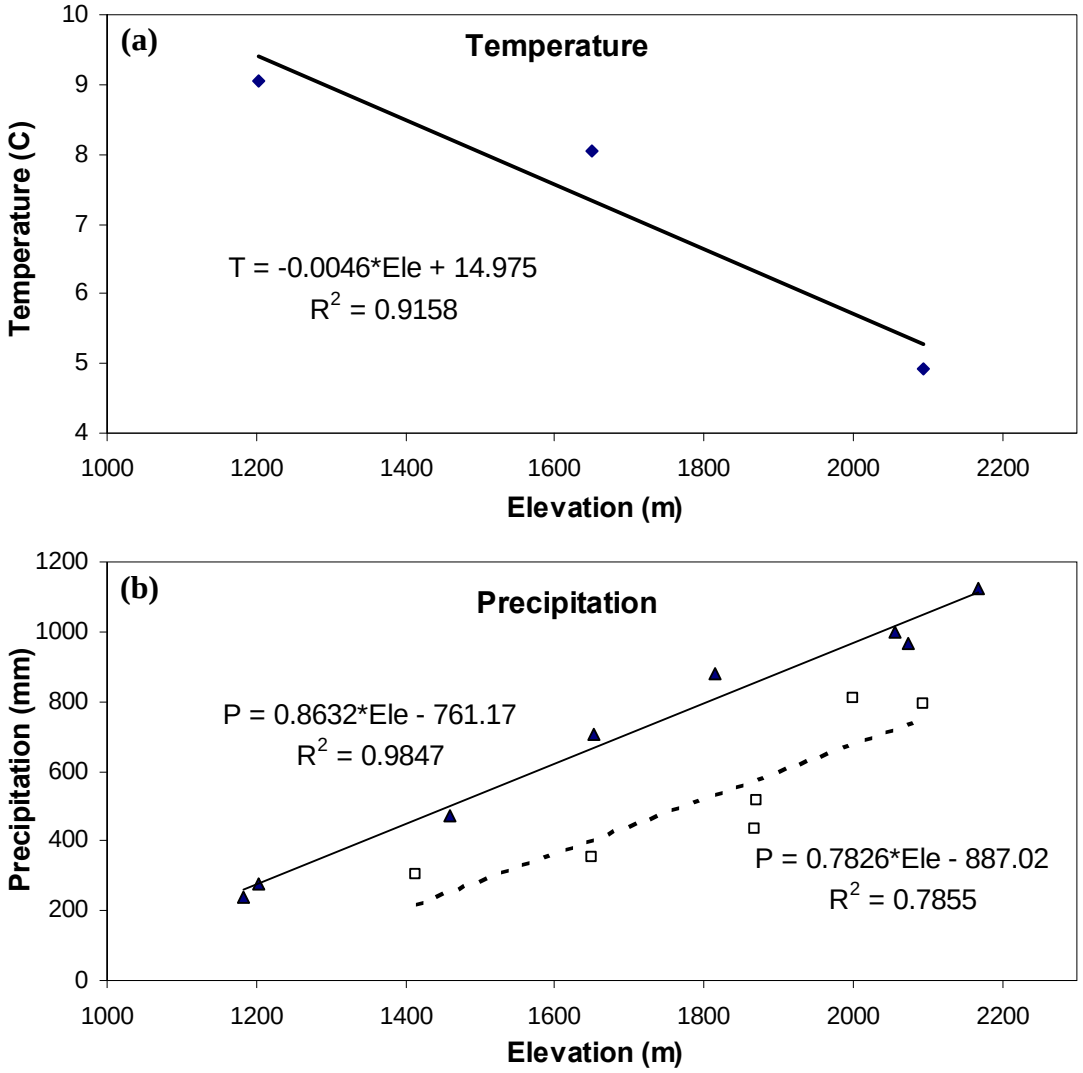

Figure 5: (a) Temperature lapse rate and (b) Precipitation lapse rate at RCEW.

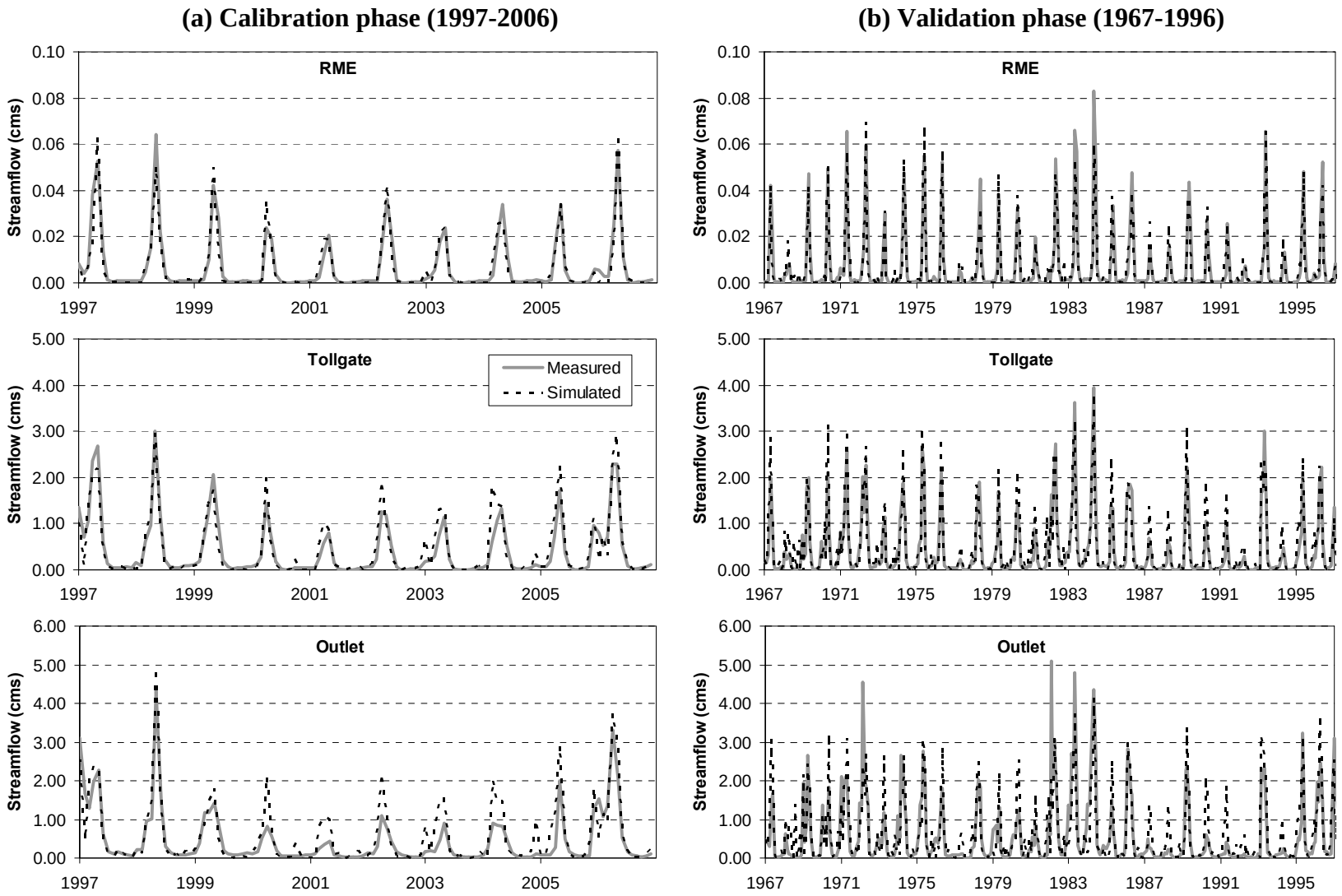

Figure 6: Comparison of observed and simulated streamflow for the three long term weirs during (a) Calibration phase (1997-2006) and (b) Validation phase (1967-1996).

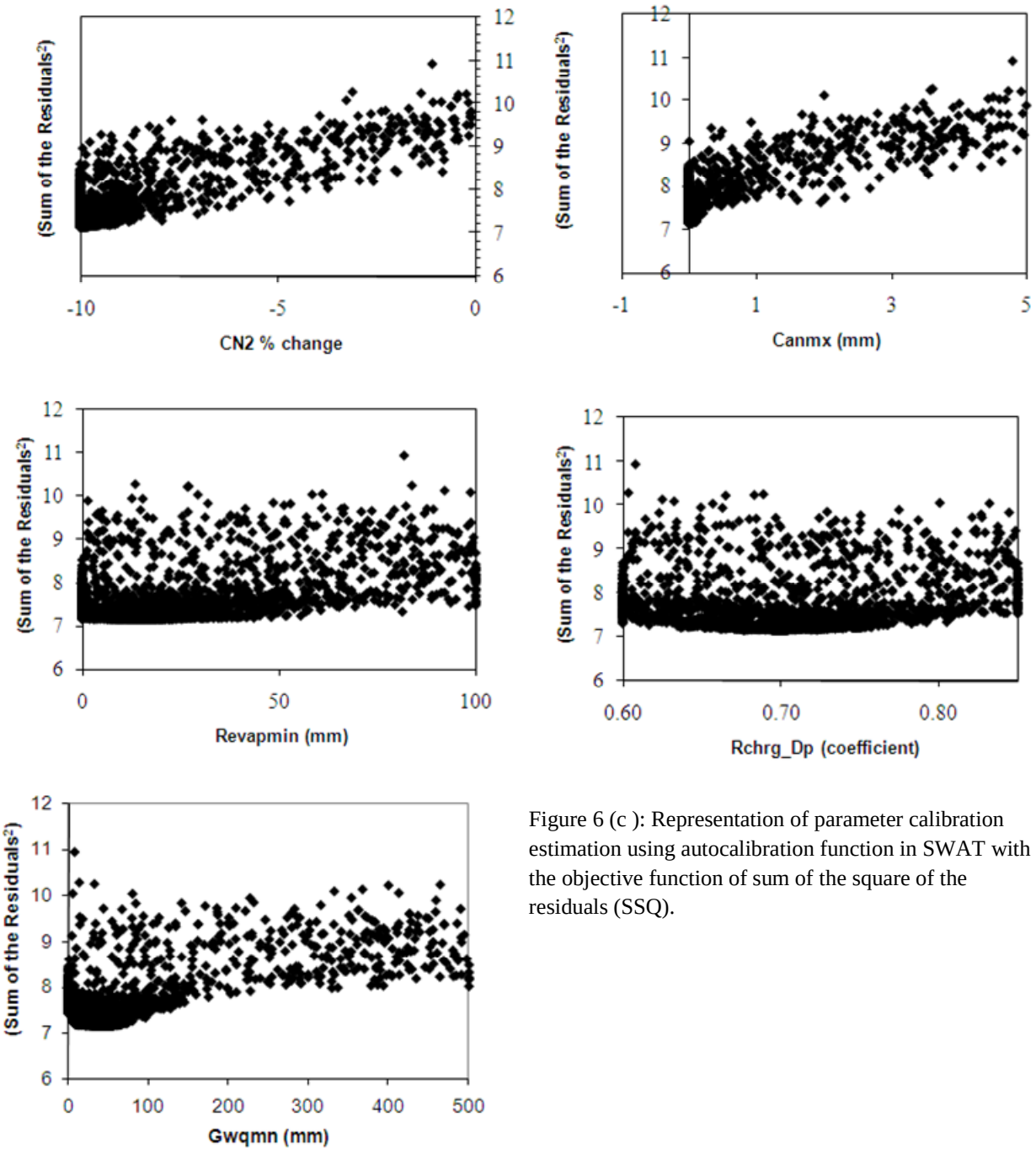

Figure 6 (c): Representation of parameter calibration estimation using autocalibration function in SWAT with the objective function of sum of the square of the residuals (SSQ).

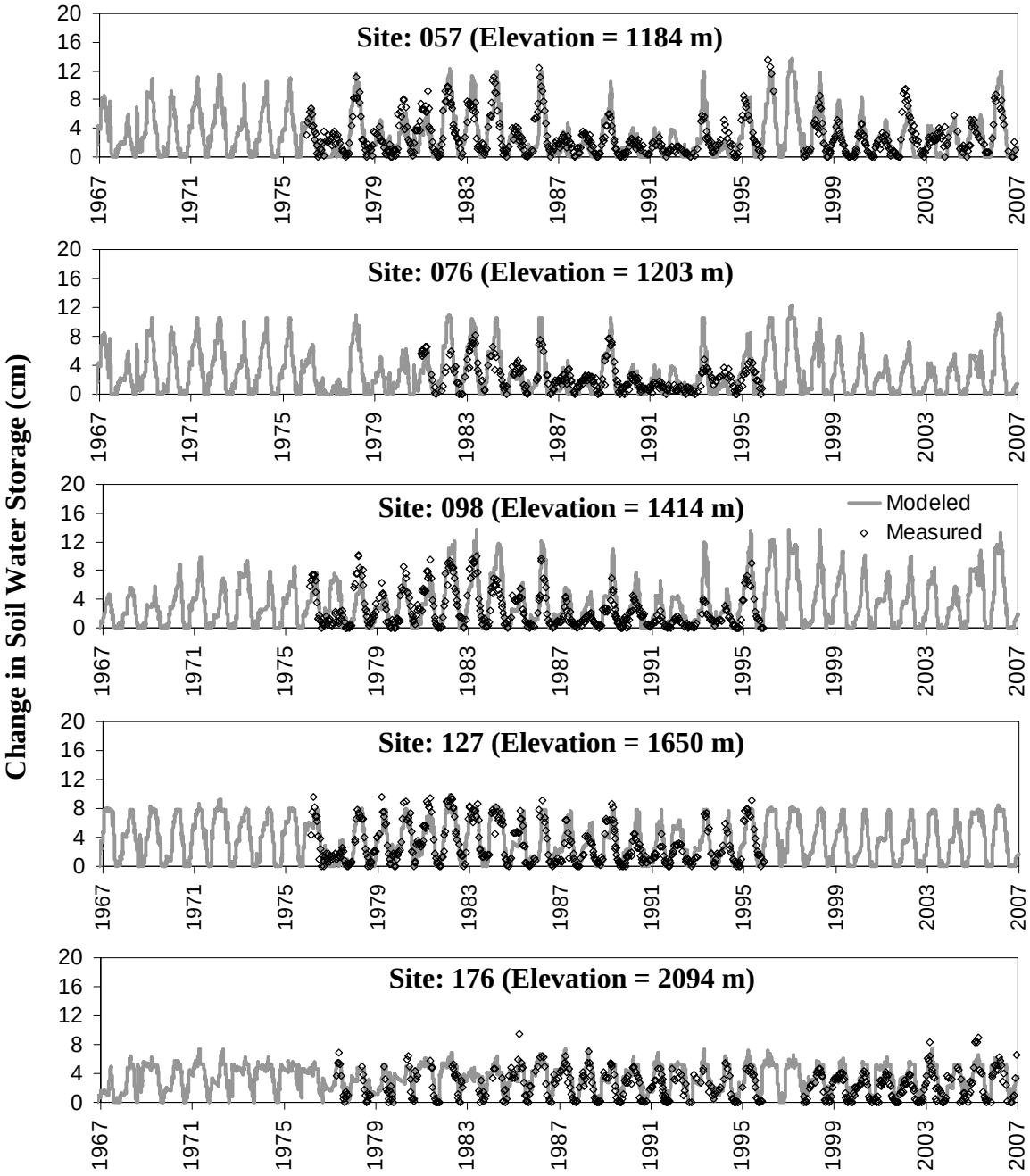

Figure 7: Comparison of measured and modeled soil water storage change at five soil moisture measurement sites and the HRUs in which they are located.

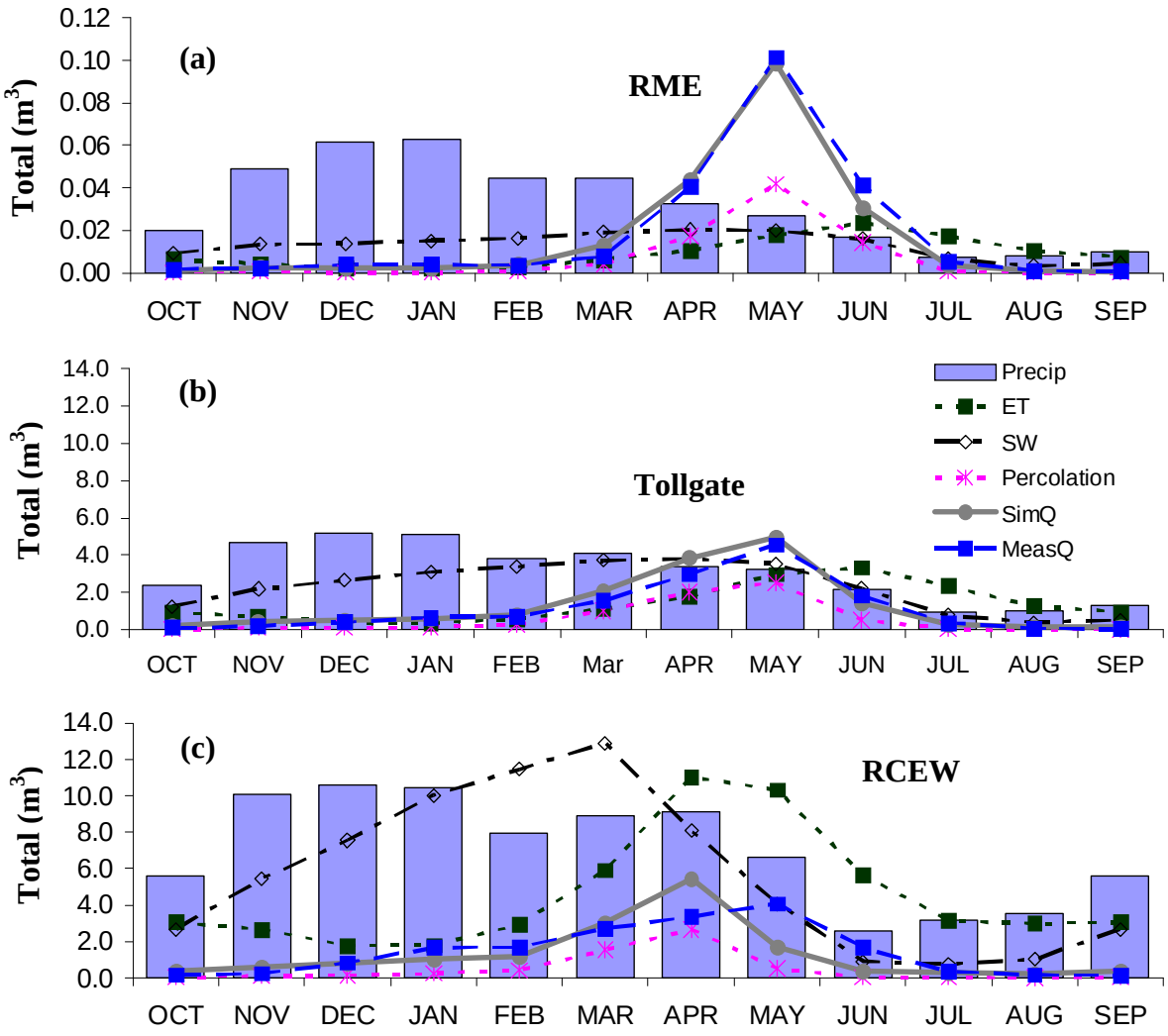

Figure 8: Average monthly water budget at (a) RME, (b) Tollgate and (c) RCEW basins, showing precipitation, evapotranspiration, soil water storage, percolation and simulated and measured streamflow.

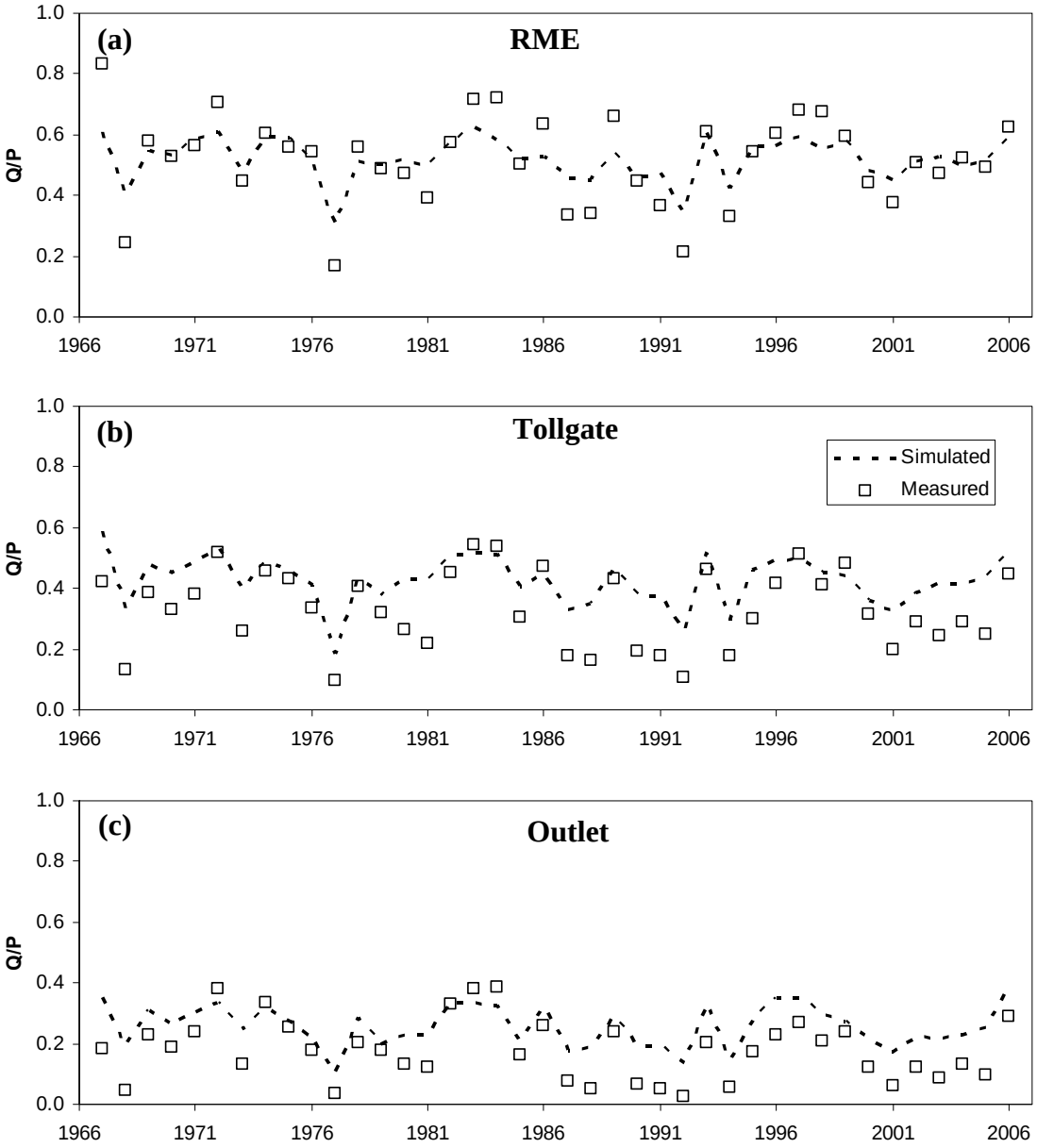

Figure 9: Comparisons of Annual Streamflow-Precipitation (Q/P) ratio for simulated and measured streamflow at (a) RME (b) Tollgate and (c) Outlet weirs.

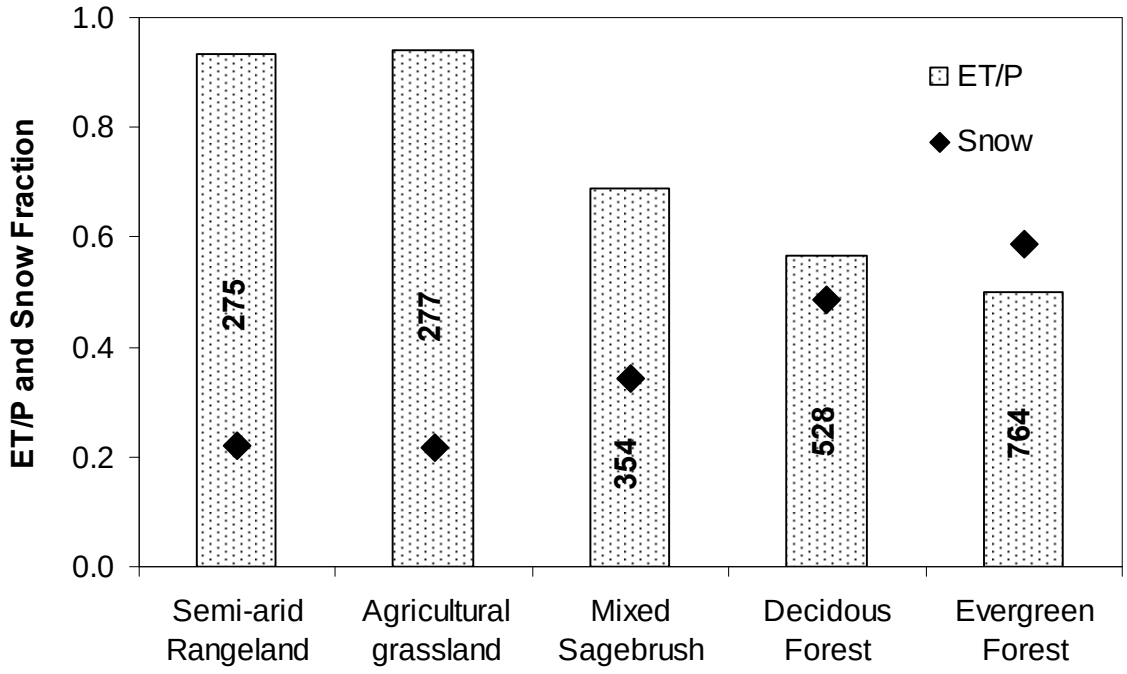

Figure 10: Evapotranspiration to precipitation (ET/P) ratio and snow fraction at each of the land use types of the RCEW. Average precipitation depth in each land cover class is shown as the numbers in the bars.

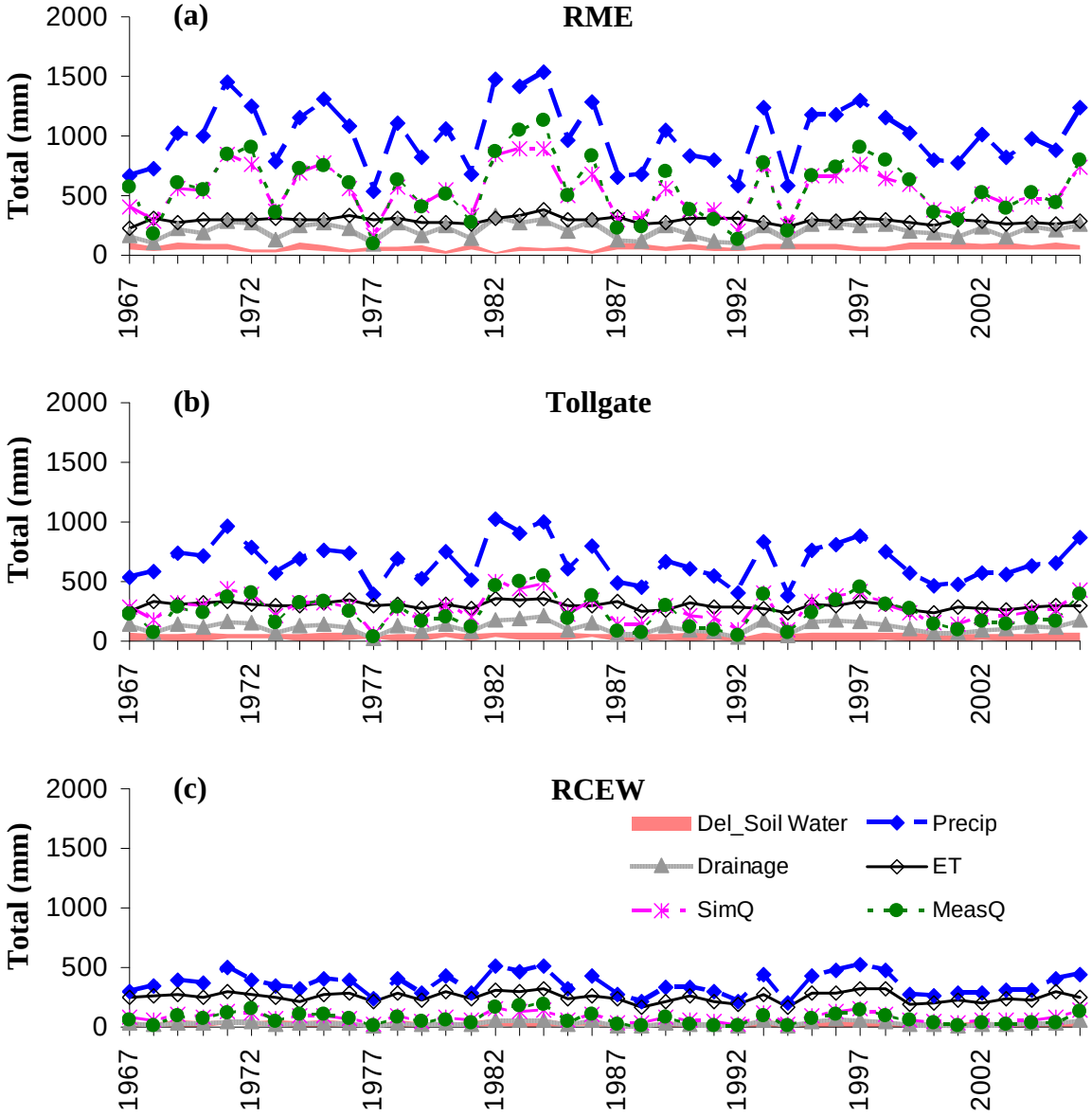

Figure 11: Annual water budget at (a) RME (b) Tollgate and (c) RCEW basins showing annual precipitation, evapotranspiration, annual change in soil water storage, deep drainage and simulated and measured streamflow.

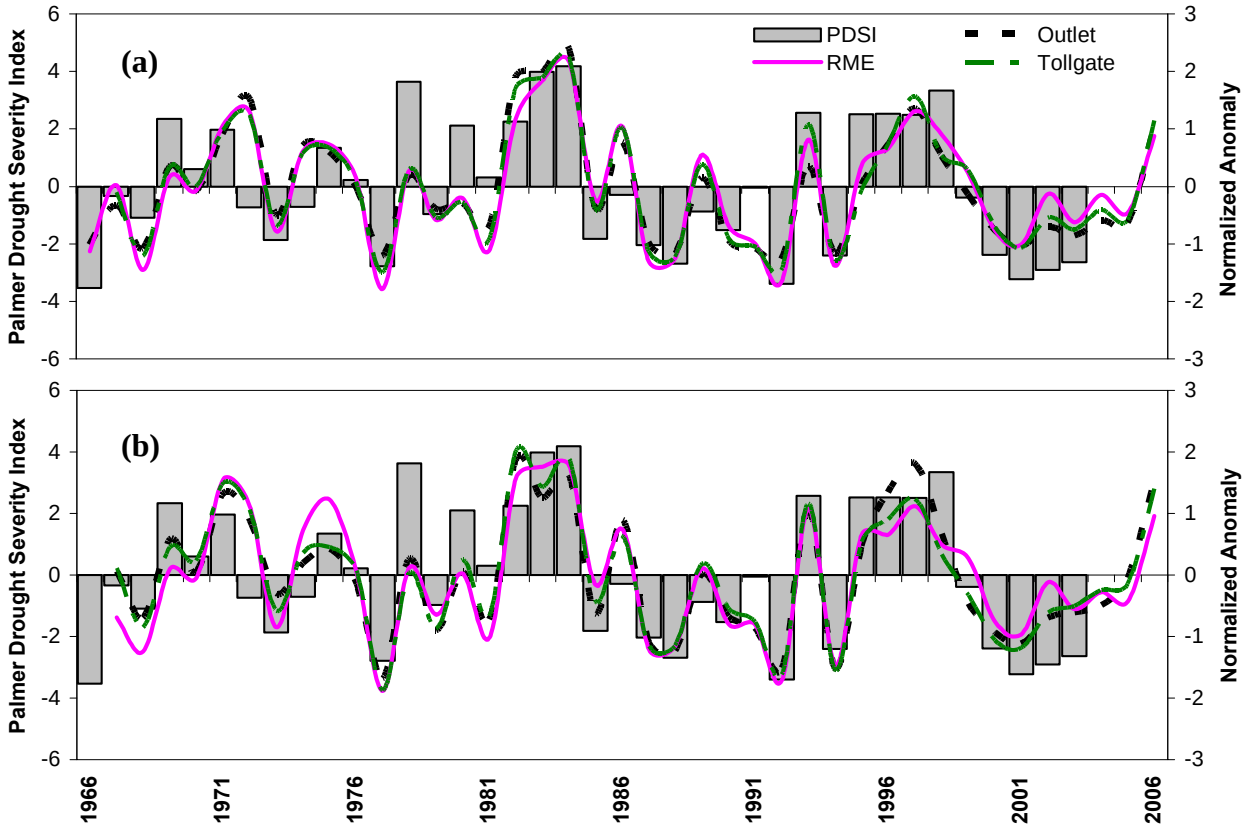

Figure 12: Palmer Drought Severity Index for RCEW and Normalized Anomaly at RME, Tollgate and Outlet weirs for (a) measured streamflow and (b) simulated streamflow.

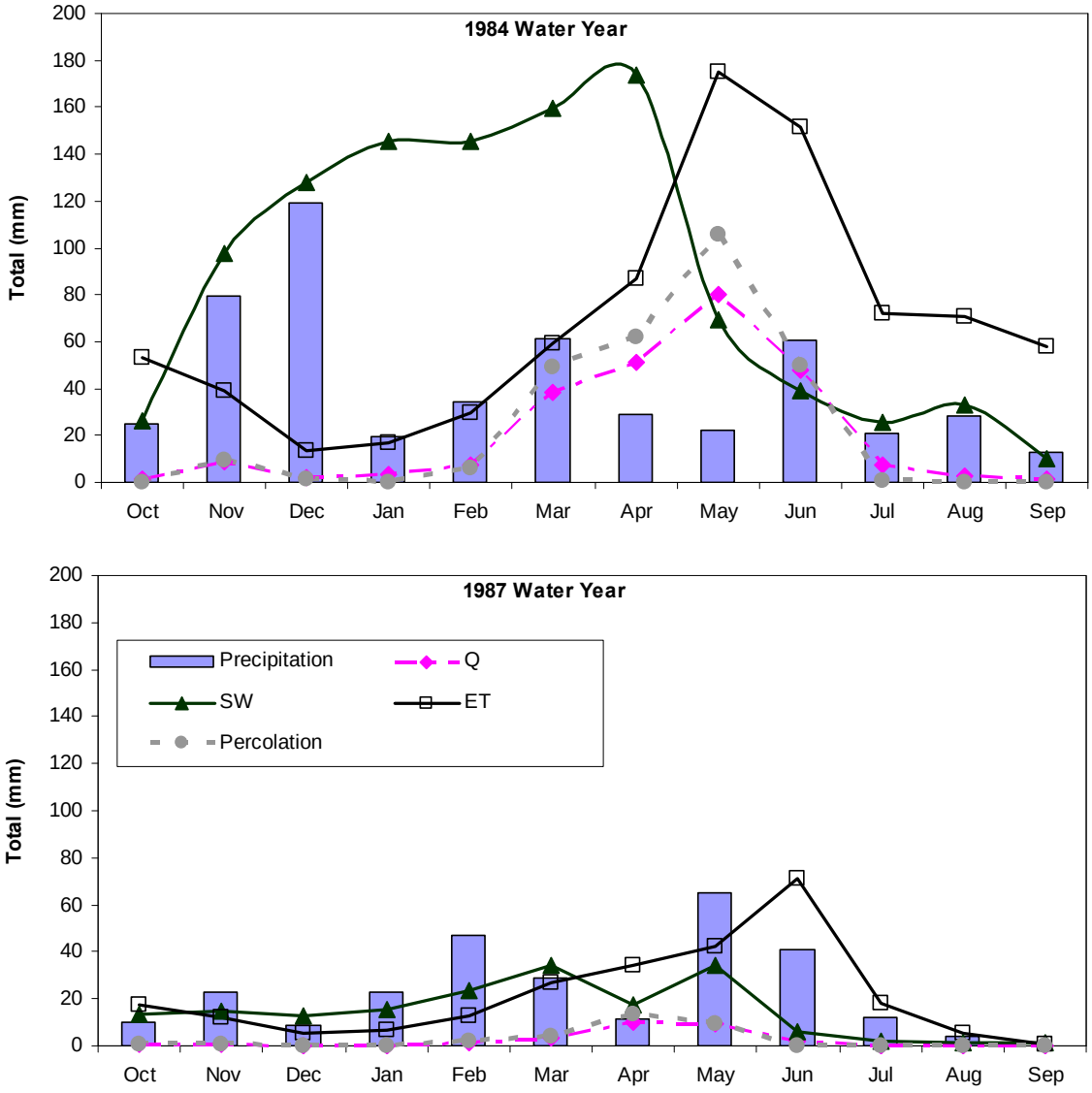

Figure 13: Monthly distribution of the water balance components during (a) wet (1984) and (b) dry water (1987) years.

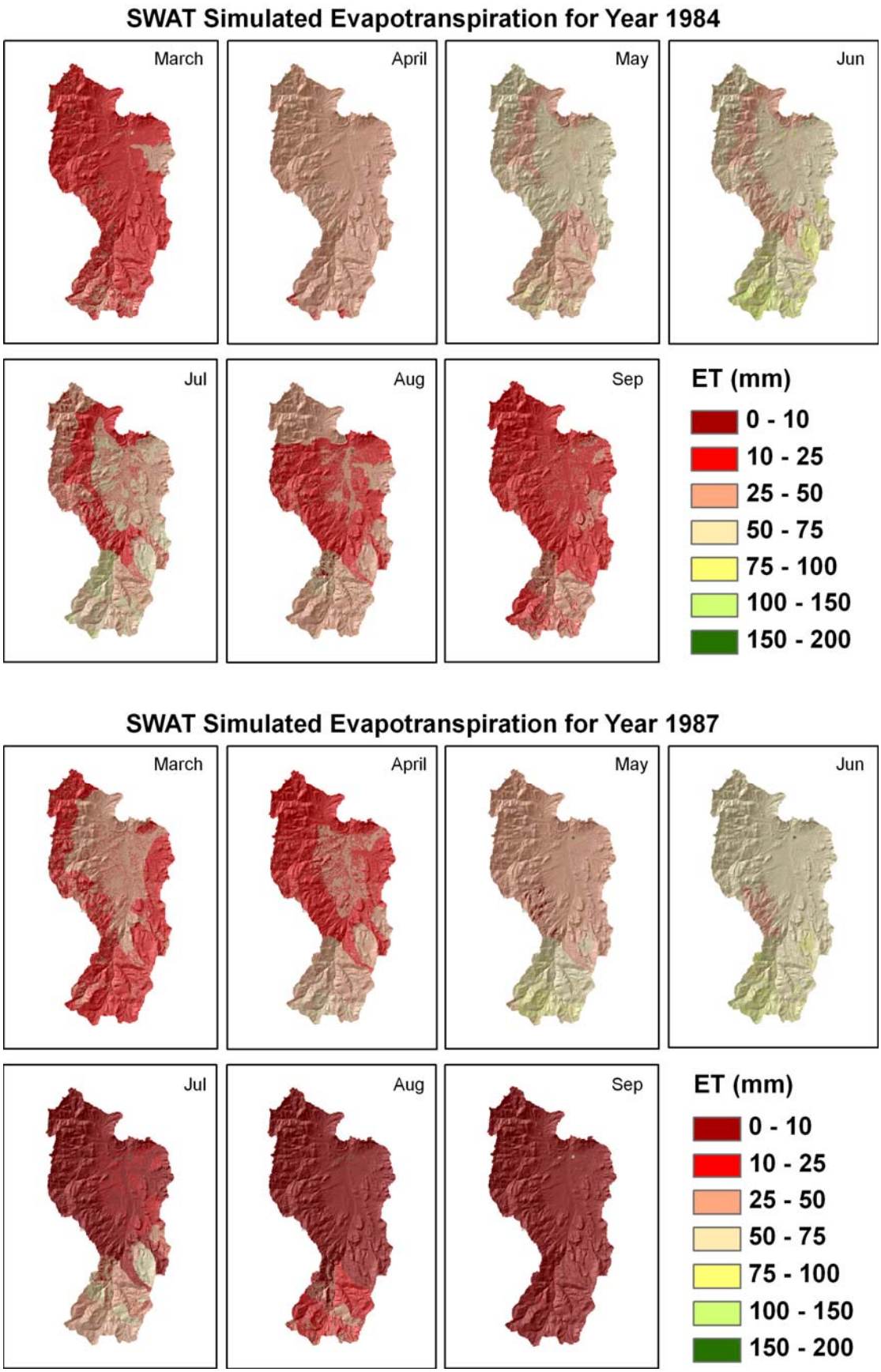

Figure 14: Simulated monthly ET distributions during wet (1984) and dry (1987) water years.

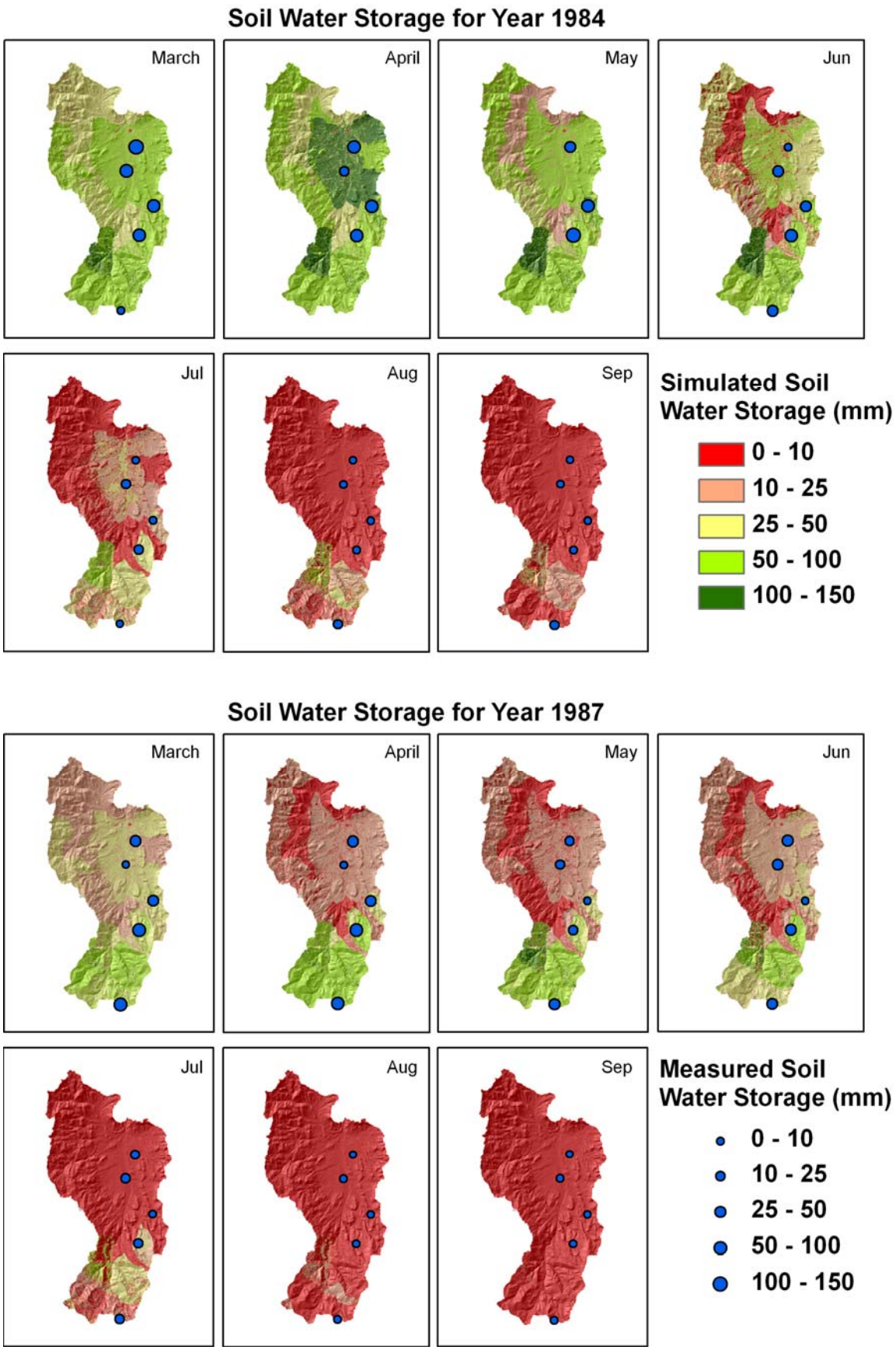

Figure 15: Simulated monthly soil water storage distributions during wet (1984) and dry (1987) water years.

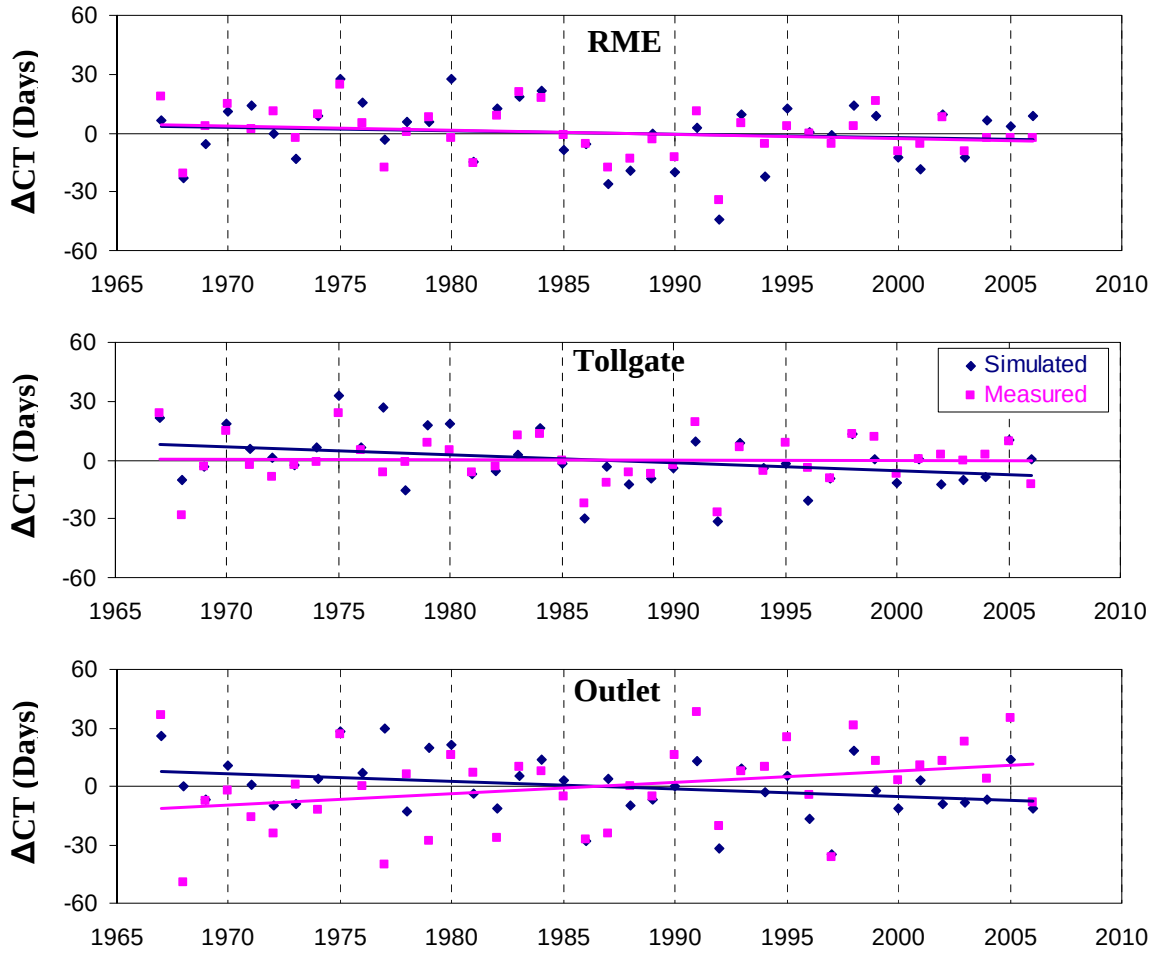

Figure 16: Simulated and Measured CT plots for the Outlet, Tollgate and RME weirs in RCEW.